


# SAUR proteins and PP2C.D phosphatases regulate H<sup>+</sup>-ATPases and K<sup>+</sup> channels to control stomatal movements

Jeh Haur Wong <sup>1,†,‡</sup> Martina Klejchová <sup>2,‡</sup> Stephen A. Snipes <sup>3,‡</sup> Punita Nagpal,<sup>3</sup>  
Gwangbae Bak <sup>3</sup> Bryan Wang,<sup>3</sup> Sonja Dunlap,<sup>1</sup> Mee Yeon Park <sup>1</sup> Emma N. Kunkel <sup>3</sup>,  
Brendan Trinidad,<sup>3</sup> Jason W. Reed <sup>3,§</sup> Michael R. Blatt <sup>2,§</sup> and William M. Gray <sup>1,\*,§</sup>

- 1 Department of Plant and Microbial Biology, University of Minnesota, St Paul, Minnesota 55108, USA
- 2 Laboratory of Plant Physiology and Biophysics, University of Glasgow, Glasgow G12 8QQ, UK
- 3 Department of Biology, University of North Carolina, Chapel Hill, North Carolina 27599-3280, USA

\*Author for communication: grayx051@umn.edu

†Present address: Department of Biological Sciences, National University of Singapore, Singapore

‡These authors contributed equally to this work.

§Co-senior authors.

W.M.G., M.R.B., and J.W.R. designed the research; J.H.W., M.K., S.A.S., P.N., S.D., M.P., G.B., B.W., E.N.K., B.T., and W.M.G. performed the experiments; W.M.G., M.R.B., and J.W.R. supervised the experiments; J.H.W., J.W.R., M.K., M.R.B., and W.M.G. wrote the article with contributions from all authors.

The author responsible for distribution of materials integral to the findings presented in this article in accordance with the policy described in the Instructions for Authors (<https://academic.oup.com/plphys>) is: William M. Gray (grayx051@umn.edu).

## Abstract

Activation of plasma membrane (PM) H<sup>+</sup>-ATPase activity is crucial in guard cells to promote light-stimulated stomatal opening, and in growing organs to promote cell expansion. In growing organs, SMALL AUXIN UP RNA (SAUR) proteins inhibit the PP2C.D2, PP2C.D5, and PP2C.D6 (PP2C.D2/5/6) phosphatases, thereby preventing dephosphorylation of the penultimate phosphothreonine of PM H<sup>+</sup>-ATPases and trapping them in the activated state to promote cell expansion. To elucidate whether SAUR–PP2C.D regulatory modules also affect reversible cell expansion, we examined stomatal apertures and conductances of *Arabidopsis thaliana* plants with altered SAUR or PP2C.D activity. Here, we report that the *pp2c.d2/5/6* triple knockout mutant plants and plant lines overexpressing SAUR fusion proteins exhibit enhanced stomatal apertures and conductances. Reciprocally, *saur56 saur60* double mutants, lacking two SAUR genes normally expressed in guard cells, displayed reduced apertures and conductances, as did plants overexpressing PP2C.D5. Although altered PM H<sup>+</sup>-ATPase activity contributes to these stomatal phenotypes, voltage clamp analysis showed significant changes also in K<sup>+</sup> channel gating in lines with altered SAUR and PP2C.D function. Together, our findings demonstrate that SAUR and PP2C.D proteins act antagonistically to facilitate stomatal movements through a concerted targeting of both ATP-dependent H<sup>+</sup> pumping and channel-mediated K<sup>+</sup> transport.

## Introduction

The stomatal pores on the epidermis of plant leaves are flanked by pairs of guard cells that swell and shrink to cause

stomatal opening and closing, respectively, thereby regulating gaseous exchange between the leaf interior and the atmosphere to support photosynthesis while minimizing

water loss through transpiration (Inoue and Kinoshita, 2017; Jezek and Blatt, 2017). Plasma membrane (PM) H<sup>+</sup>-ATPases play an important role in stomatal aperture regulation. These H<sup>+</sup>-ATPases are activated in response to red and blue light, energizing the guard cell PM by transporting protons into the apoplast (Kinoshita and Shimazaki, 1999; Inoue and Kinoshita, 2017; Ando and Kinoshita, 2018) to generate a H<sup>+</sup> electrochemical gradient across the PM and negative membrane voltage. Membrane energization powers ion flux, notably through inward-rectifying K<sup>+</sup> and Cl<sup>-</sup> channels to drive solute and water into guard cells, generating turgor pressure and an increase in guard cell volume to open the stomatal pore (Chen et al., 2012; Hills et al., 2012; Minguet-Parramona et al., 2016).

During stomatal opening, guard cells accumulate solutes, mainly K<sup>+</sup>, Cl<sup>-</sup>, malate, and sugar (Jezek and Blatt, 2017). The negative membrane voltage activates inward-rectifying K<sup>+</sup> channels, primarily K<sup>+</sup> CHANNEL IN ARABIDOPSIS THALIANA (KAT1), to promote K<sup>+</sup> influx (Nakamura et al., 1995; Pilot et al., 2001, 2003; Lebaudy et al., 2008). Proton-coupled K<sup>+</sup> transport via HIGH AFFINITY K<sup>+</sup>-type transporters also contributes to K<sup>+</sup> accumulation (Blatt and Slayman, 1987; Blatt and Clint, 1989; Maathuis and Sanders, 1994; Osakabe et al., 2013; Véry et al., 2014). During stomatal closing, H<sup>+</sup>-ATPase activity is suppressed and Cl<sup>-</sup> channels are activated to promote membrane depolarization, thereby suppressing K<sup>+</sup> uptake through inward-rectifying K<sup>+</sup> channels and promoting K<sup>+</sup> efflux through outward-rectifying K<sup>+</sup> channels, including the gated outwardly-rectifying K<sup>+</sup> (GORK) channel of Arabidopsis (Jezek and Blatt, 2017). Such changes in ion flux are evident also in response to abscisic acid (ABA; Blatt, 1990; Linder and Raschke, 1992). ABA promotes an increase in cytosolic free calcium ([Ca<sup>2+</sup>]<sub>i</sub>) by triggering Ca<sup>2+</sup> influx and its release via endomembrane Ca<sup>2+</sup> channels (Grabov and Blatt, 1997, 1998, 1999; Hamilton et al., 2000; Garcia-Mata et al., 2003). The increase of [Ca<sup>2+</sup>]<sub>i</sub>, together with ABA-mediated activation of SLAC (S-type) and ALMT (R-type) anion channels, leads to anion efflux and reduced PM H<sup>+</sup>-ATPase activity, resulting in membrane depolarization (Schmidt et al., 1995; Grabov and Blatt, 1997; Merlot et al., 2007; Geiger et al., 2009; Chen et al., 2010; Meyer et al., 2010). The elevated [Ca<sup>2+</sup>]<sub>i</sub> also prevents K<sup>+</sup> uptake by suppressing inward-rectifying K<sup>+</sup> channels (KAT1; Grabov and Blatt, 1997, 1999) and GORK channel activity is further enhanced by increased cytosolic pH (pH<sub>i</sub>; Blatt, 1990; Blatt and Armstrong, 1993; Grabov and Blatt, 1997; Suhita et al., 2004).

In our prior work on auxin-mediated cell expansion, we found that members of the PP2C.D family of type 2C protein phosphatases repress cell expansion by dephosphorylating PM H<sup>+</sup>-ATPases to inhibit H<sup>+</sup> pumping activity (Spartz et al., 2014; Ren et al., 2018; Du et al., 2020). Several SMALL AUXIN UP RNA (SAUR) proteins antagonize PP2C.D activity by binding these phosphatases to inhibit their enzymatic activity, thereby promoting cell expansion (Spartz et al., 2014, 2017; Ren et al., 2018). Given that PM H<sup>+</sup>-ATPases are

critical regulators of both cell expansion and stomatal aperture control, we examined whether similar SAUR–PP2C.D regulatory modules might also govern stomatal movements. Our prior findings hinted at this possibility, as both Arabidopsis and tomato (*Solanum lycopersicum*) plants ectopically expressing SAUR19 fusion proteins driven by the Cauliflower mosaic virus 35S promoter exhibited reduced drought tolerance (Spartz et al., 2014, 2017). Although SAUR19 is not normally expressed in guard cells and is therefore unlikely to regulate stomatal movements, several other SAUR and PP2C.D phosphatase genes are expressed in guard cells (Bauer et al., 2013; Adrian et al., 2015), supporting the possibility that SAUR–PP2C.D modules may play a role in stomatal function.

Here we report that SAUR proteins and PP2C.D phosphatases regulate stomatal aperture in Arabidopsis. Similar to their roles in controlling cell expansion during organ growth, SAUR and PP2C.D proteins function antagonistically in guard cells, with SAURs inhibiting PP2C.D activity to promote stomatal opening and conductance. Although these findings are consistent with SAUR–PP2C.D modules controlling stomatal aperture via the PM H<sup>+</sup>-ATPases, voltage clamp analysis in plants with perturbed SAUR or PP2C.D function uncovered substantial changes in the activities of both inward- and outward-rectifying K<sup>+</sup> channels, including a dramatic effect on voltage-dependence of gating of the outward-rectifying K<sup>+</sup> channels of guard cells. Thus, our findings indicate that SAUR–PP2C.D control modules target multiple transport processes to govern stomatal movements.

## Results

### Gain-of-function SAUR fusion proteins increase stomatal apertures

We previously noticed that plants expressing 35S:GFP-SAUR19 or 35S:StreptII-SAUR19 transgenes exhibited larger stomatal apertures and accelerated water loss compared to the wild-type (Spartz et al., 2014, 2017). To determine if these phenotypes were a general property of SAUR overexpression, we conducted water loss assays on plants overexpressing a SAUR63-YFP-HA fusion protein. SAUR63 and SAUR19 represent distinct clades of the 79-member Arabidopsis SAUR gene family. Although distantly related to one another (Ren and Gray, 2015), they share the highly conserved 60–70 amino acid core SAUR domain and both are stabilized as xFP-fusion proteins to cause a gain of function (Chae et al., 2012; Spartz et al., 2012). As previously observed with SAUR19 overexpression lines (Spartz et al., 2014, 2017), detached leaves of SAUR63-YFP-HA overexpression plants lost water faster than did leaves of wild-type controls (Figure 1A). The water loss phenotype is similar to the dominant *open stomata2* (*ost2-2*) mutant, which harbors two-point mutations (L<sub>169</sub>F and G<sub>867</sub>S) in AUTOINHIBITED H<sup>+</sup> ATPASE (*AHA1*) that confer constitutive proton pump activity (Merlot et al., 2007).

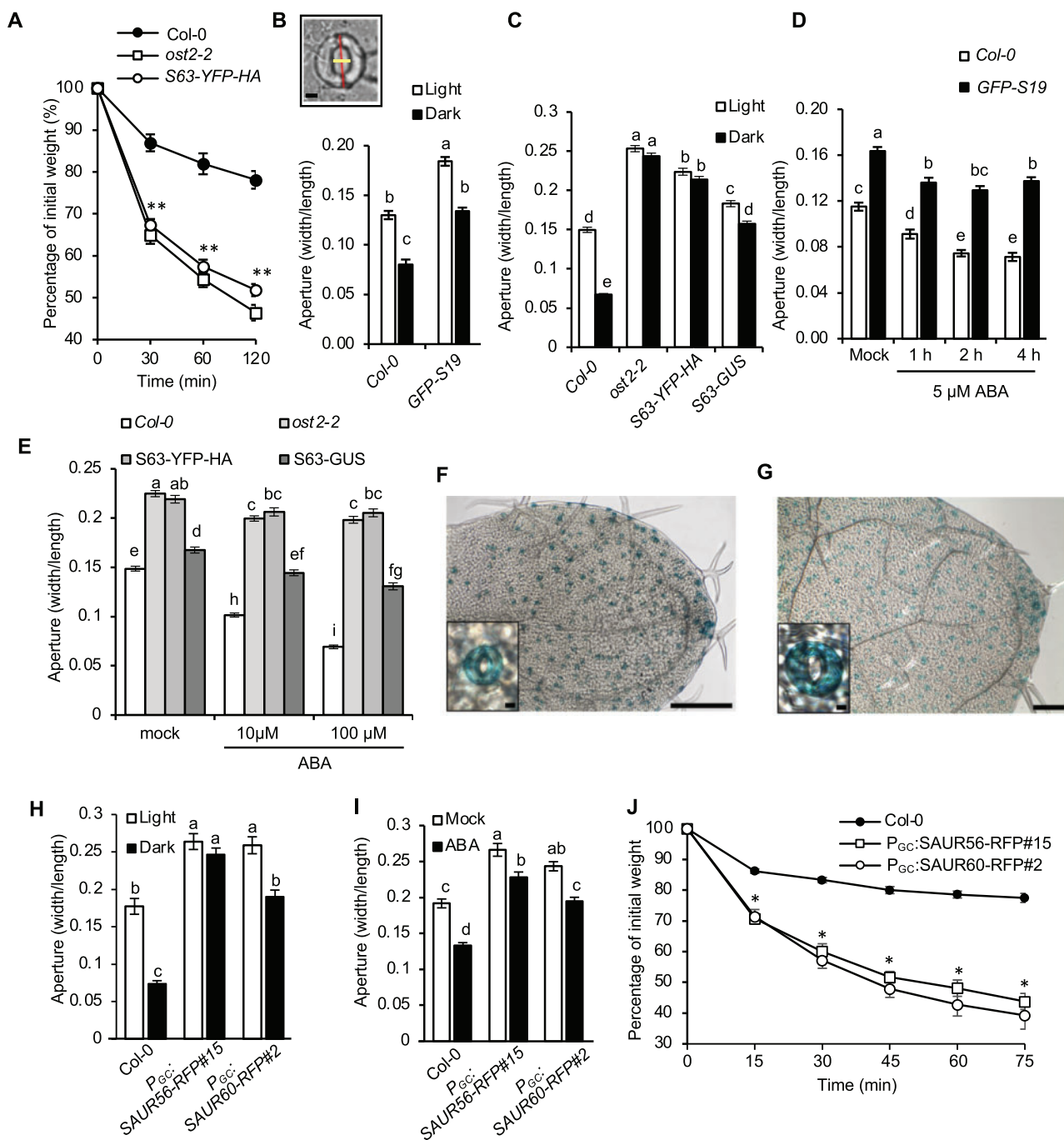


**Figure 1** SAUR overexpression confers larger stomatal aperture. (A) Water loss in leaf detachment assays of wild-type Col-0, *ost2-2*, and 35S:SAUR63-YFP-HA plants. Data are means  $\pm$  SE ( $n = 15$ ). (B) Stomatal aperture measurements of wild-type Col-0 and 35S:GFP-SAUR19 plants during light and dark conditions for 2 h. Data are means  $\pm$  SE ( $n = 60$ ). Inset depicts aperture width/length stomate measurements. Scale bar = 5  $\mu$ m. (C) Stomatal aperture measurements of wild-type Col-0, *ost2-2*, 35S:SAUR63-YFP-HA, and 35S:SAUR63-GUS plants during light and dark conditions for 2 h. Data are means  $\pm$  SE ( $n \geq 106$ ). (D) Stomatal aperture measurement of wild-type Col-0 and 35S:GFP-SAUR19 plants following treatment with 5  $\mu$ M ABA. Data are means  $\pm$  SE ( $n = 60$ ). (E) Stomatal aperture measurements of wild-type, *ost2-2*, 35S:SAUR63-YFP-HA, and 35S:SAUR63-GUS after 1h treatments with 10 or 100  $\mu$ M ABA. Data are means  $\pm$  SE ( $n \geq 113$ ). X-Gluc staining of young leaves from *P<sub>SAUR56</sub>:SAUR56-GUS* (F) and *P<sub>SAUR60</sub>:GUS* (G) seedlings. Scale bars = 250  $\mu$ m (whole leaf), 5  $\mu$ m (inset). Stomatal aperture measurements of wild-type, *P<sub>GC</sub>:SAUR56-RFP*, and *P<sub>GC</sub>:SAUR60-RFP* plants during light and dark conditions ( $n \geq 48$ ) (H) or following a 1 h treatment with 100  $\mu$ M ABA ( $n \geq 65$ ) (I). (J) Water loss in leaf detachment assays of wild-type, *P<sub>GC</sub>:SAUR56-RFP* and *P<sub>GC</sub>:SAUR60-RFP* plants. Data are means  $\pm$  SE ( $n = 6$ ). All experiments were repeated at least twice with similar results. Different letters above error bars indicate significant difference ( $P < 0.05$ ) by one-way analysis of variance analysis with Tukey's HSD test. (A and J) Asterisks indicate significant difference from the wild-type ( $P < 0.05$ , Student's *t* test).



We examined stomatal responses to light and dark treatments after pre-incubating epidermal peels to induce stomatal opening. Protocols for these experiments differed slightly between our laboratories (see Materials and methods section), but yielded similar results, confirming the robustness of these phenotypes. Plants harboring *35S::GFP-SAUR19* or *35S::StreptII-SAUR19* overexpression constructs exhibited larger stomatal apertures than did wild-type plants under both light and dark conditions (Figure 1B; Supplemental Figure S1A). Likewise, plants overexpressing *SAUR63-YFP-HA* or *-GUS* fusion proteins also displayed increased aperture diameter (Figure 1C). Similarly, compared to the wild-type control, *SAUR19* and *SAUR63* overexpression lines displayed reduced aperture closing in response to ABA (Figure 1, D and E; Supplemental Figure S1B).

Guard cells in the *SAUR19* and *SAUR63* overexpression lines were also larger than Col-0 guard cells (Supplemental Figure S1, C and D), reflecting roles for these proteins in promoting cell expansion during growth (Chae et al., 2012; Spartz et al., 2012, 2014). To confirm that the aperture phenotypes exhibited by *SAUR* overexpressors were due to altered guard cell responsiveness, we measured the apertures of estradiol-inducible *SAUR63-CeruleanFP-HA* ( $P_{EST::SAUR63-CerFP-HA}$ ) leaves subjected to a 1 h, 5  $\mu$ M ABA treatment. Apertures of uninduced  $P_{EST::SAUR63-CerFP-HA}$  stomata were comparable to Col-0 controls and closed in response to ABA (Supplemental Figure S1E). In contrast, induction of *SAUR63-CerFP-HA* expression with 10  $\mu$ M estradiol for 1 h increased the aperture diameter of  $P_{EST::SAUR63-CerFP-HA}$  stomata, and largely prevented closure in response to ABA (Supplemental Figure S1E). These findings indicate a significant effect on aperture regulation, and are supported by kinetic analysis of stomatal conductances (below).

We used reverse transcription-PCR (RT-PCR) to examine the expression of *SAUR* genes in guard cells, comparing data from isolated guard cell protoplasts (GCPs) to that from whole Arabidopsis leaves. This analysis revealed that although neither *SAUR19* nor *SAUR63* was expressed in guard cells, expression of several other *SAUR* family members was observed (Supplemental Figure S2A). These findings are consistent with prior transcriptomic studies (Yang et al., 2008; Wang et al., 2011; Bauer et al., 2013). *SAUR56* and *SAUR60* comprise a subclade in the phylogeny of Arabidopsis *SAUR* proteins (Ren and Gray, 2015), and expression of both genes is repressed by ABA, suggesting a possible role in stomatal aperture control (Bauer et al., 2013). To examine the expression of these *SAUR* genes,  $P_{SAUR56::SAUR56-GUS}$  and  $P_{SAUR60::GUS}$  reporter constructs were transformed into wild-type Arabidopsis plants. Both reporters were expressed specifically in the guard cells of cotyledons and leaves, and could not be detected in other shoot cells examined (Figure 1, F and G; Supplemental Figure S2, B and C).

To test whether *SAUR* proteins that are normally expressed in guard cells could also promote stomatal opening, we made  $P_{GC::SAUR56-RFP}$  and  $P_{GC::SAUR60-RFP}$  plants, expressing putative gain-of-function fusion proteins under

the control of an ABA-insensitive form of the guard cell-specific *pMYB60* promoter ( $P_{GC}$ ; Cominelli et al., 2005, 2011).  $P_{GC::SAUR56-RFP}$  and  $P_{GC::SAUR60-RFP}$  lines each had more open stomata than did the wild-type in the light, after shift to darkness, and after treatment with ABA (Figure 1, H and I; Supplemental Figure S2, D and E), similarly to the *SAUR19* and *SAUR63* overexpression lines. Detached leaves of these plants also lost water faster than did wild-type leaves (Figure 1J). Thus, both the native *SAUR* proteins and ectopically expressed *SAURs* promote an increase in stomatal aperture under a variety of conditions.

### Several PP2C.D proteins repress stomatal opening

We hypothesized that the more open stomatal aperture phenotypes of the *SAUR* overexpression lines might be due to inhibition of PP2C.D activity. To explore this possibility, we first examined the expression of PP2C.D phosphatase genes in guard cells. RT-PCR assays were carried out as before to compare the expression from GCPs and from intact leaves. With the exception of *PP2C.D1*, substantial expression of all PP2C.D family members was detected in the guard cells (Supplemental Figure S3A). Largely consistent with this finding,  $\beta$ -glucuronidase (GUS) staining of leaf epidermal peels of Arabidopsis plants expressing native PP2C.D promoter-driven GUS reporter constructs (Ren et al., 2018) was evident for all PP2C.D family members except *PP2C.D1* and *D7* (Figure 2, A; Supplemental Figure S3B).

Of the nine Arabidopsis PP2C.D phosphatases, the PM-localized *PP2C.D2*, *PP2C.D5*, and *PP2C.D6* subset (hereafter denoted as *PP2C.D2/5/6*) inhibit PM  $H^+$ -ATPase activity to repress organ growth (Ren et al., 2018). Among these family members, *PP2C.D6* was strongly expressed in guard cells, with *PP2C.D2* and *D5* expressed to a lesser extent (Figure 2A). Confocal imaging of *PP2C.D2/5/6-GFP* fusion proteins driven by their native promoters confirmed their localization at the periphery of the guard cells (Figure 2B), much as reported in other cell types (Tovar-Mendez et al., 2014; Ren et al., 2018).

To test whether *PP2C.D2/5/6* normally regulate stomatal aperture, we assayed water loss from detached leaves from single-, double-, and triple-mutant combinations. None of the single mutants exhibited an obvious difference from the wild-type, whereas the *pp2c.d2/6* and *d5/6* double mutants displayed a slight increase in the rate of water loss (Supplemental Figure S4A). The *pp2c.d2/5/6* triple mutant exhibited an even greater increase in water loss, similar to those of *35S::GFP-SAUR19*, *35S::SAUR63-YFP-HA*,  $P_{GC::SAUR56-RFP}$ ,  $P_{GC::SAUR60-RFP}$  and *ost2-2* plants (Figures 1, A, J and 2, C; Supplemental Figure S4A).

We next examined stomatal apertures in the *pp2c.d2/5/6* triple mutants. Under both light and dark conditions, the triple mutant exhibited larger apertures than the wild-type (Figure 2D). When treated with 5  $\mu$ M ABA to induce closing, stomata of the *pp2c.d2/5/6* mutant displayed both slower kinetics and a reduction in closure compared to the wild-type control (Figure 2E). The aperture phenotype of *pp2c.d2/5/6* mutants was complemented by *PP2C.D5-GFP*,

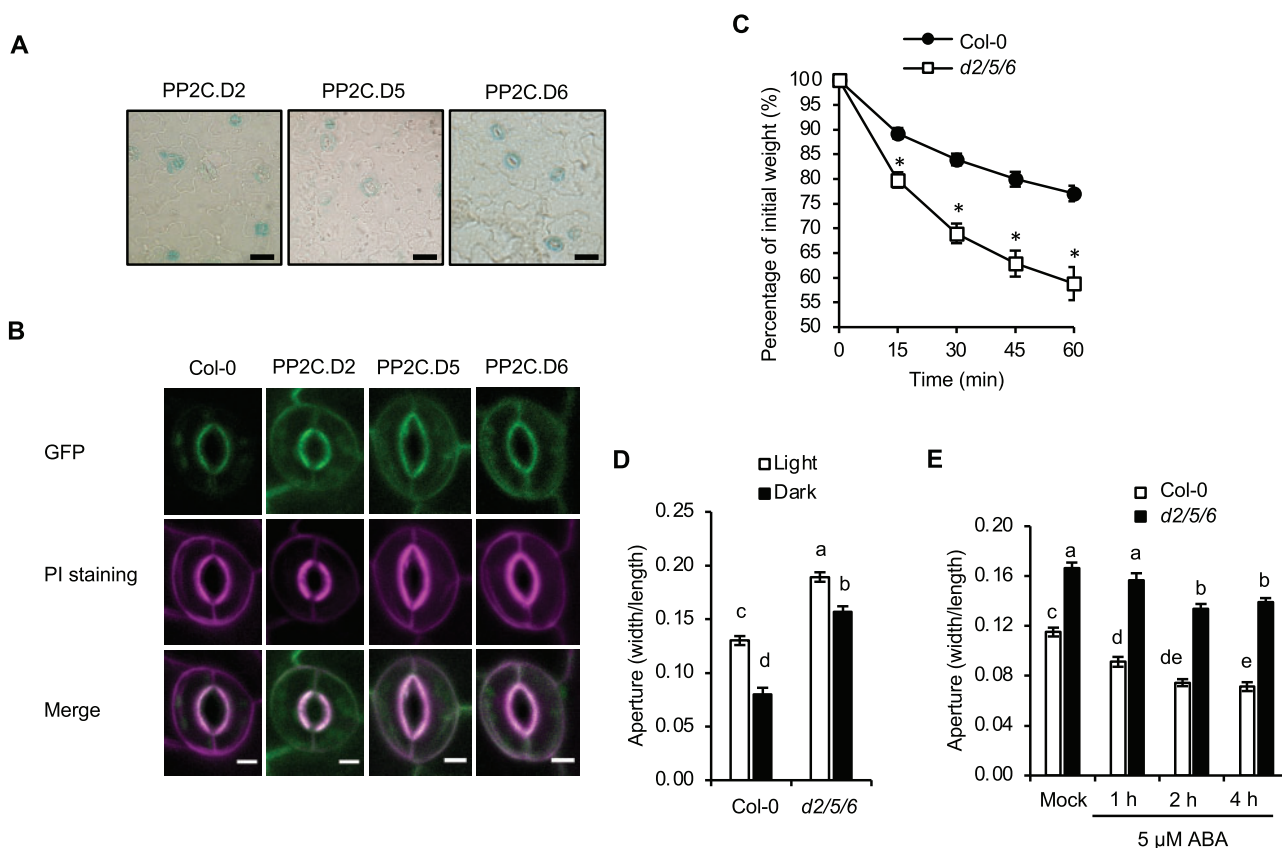


**Figure 2** The *pp2c.d2/5/6* triple mutant exhibits increased stomatal aperture diameter. **(A)** X-Gluc staining of native promoter:PP2C.D-GUS translational fusion proteins in leaf epidermal peels. Scale bar = 25  $\mu\text{m}$ . **(B)** Subcellular localization of native promoter:PP2C.D-GFP fusion proteins (green) in guard cells of 7-d-old cotyledons. Propidium iodide (PI) (magenta) was used to mark the cell periphery. Scale bar = 5  $\mu\text{m}$ . **(C)** Water loss in leaf detachment assays of wild-type Col-0 and *pp2c.d2/5/6* triple mutants. Data are means  $\pm$  SE ( $n = 8$ ). Asterisks indicate significant difference from the wild-type ( $P < 0.05$ , Student's  $t$  test). **(D)** Stomatal aperture measurements of wild-type Col-0 and *pp2c.d2/5/6* triple mutants during light and dark conditions for 2 h. Data are means  $\pm$  SE ( $n = 60$ ). **(E)** Stomatal aperture measurements of the wild-type and *pp2c.d2/5/6* triple mutants following treatment with 5  $\mu\text{M}$  ABA. Data are means  $\pm$  SE ( $n = 60$ ). Different letters above error bars indicate significant difference ( $P < 0.05$ ) by one-way analysis of variance analysis with Tukey's HSD test.

PP2C.D6-GFP, and to lesser extent, PP2C.D2-GFP transgenes (Supplemental Figure S4, B–D). Thus, we conclude that PP2C.D2, PP2C.D5, and PP2C.D6 act redundantly to inhibit stomatal opening, as they also do in inhibiting cell growth (Ren et al., 2018).

### SAUR overexpression and *pp2c.d2/5/6* mutant lines exhibit abnormal stomatal kinetics

We examined stomatal kinetics of SAUR19/63 overexpressors and *pp2c.d2/5/6* mutants during dark/light/dark transitions using infrared gas analysis to determine the stomatal conductance ( $g_s$ ; Merlot et al., 2007; Wang et al., 2012, 2017). Plants were pre-adapted to the dark and  $g_s$  was determined on stepping to 400  $\mu\text{mol m}^{-2} \text{s}^{-1}$  light and on return to the dark (Figure 3A). The kinetics of stomatal opening was fitted to an exponential function of the following form:

$$y = y_0 + a(1 - e^{-bt}) \quad (1)$$

where  $y_0$  is the value of conductance at time 0,  $a$  is the range of conductance,  $b$  is the apparent rate constant of the

relaxation, and  $t$  is the time from the start of the light period. The steady-state value of  $g_s$  for the open stomata is defined by the value ( $y_0 + a$ ) and for the closed stomata by the value  $y_0$ . We found that the *pp2c.d2/5/6* mutant and SAUR19/63 overexpressors exhibited increased  $g_s$  at all times (Figure 3, A and B). The opening kinetics were also slowed in comparison to the wild-type (Figure 3C).

For the measurement of stomatal closure kinetics, plants were returned to dark conditions, and conductance curves were fitted with an exponential decay function of the following form:

$$y = y_0 + ae^{-bt} \quad (2)$$

where the parameters have the same meanings as before. Once again, the *pp2c.d2/5/6* mutant and SAUR overexpressor lines exhibited greater baseline values for  $g_s$  compared with the wild-type (Figure 3A) and, similarly, the triple mutant and SAUR overexpressors displayed slower closure kinetics (Figure 3D). Thus, we concluded that the *pp2c.d2/5/6* mutant and SAUR19/63 overexpression lines were affected

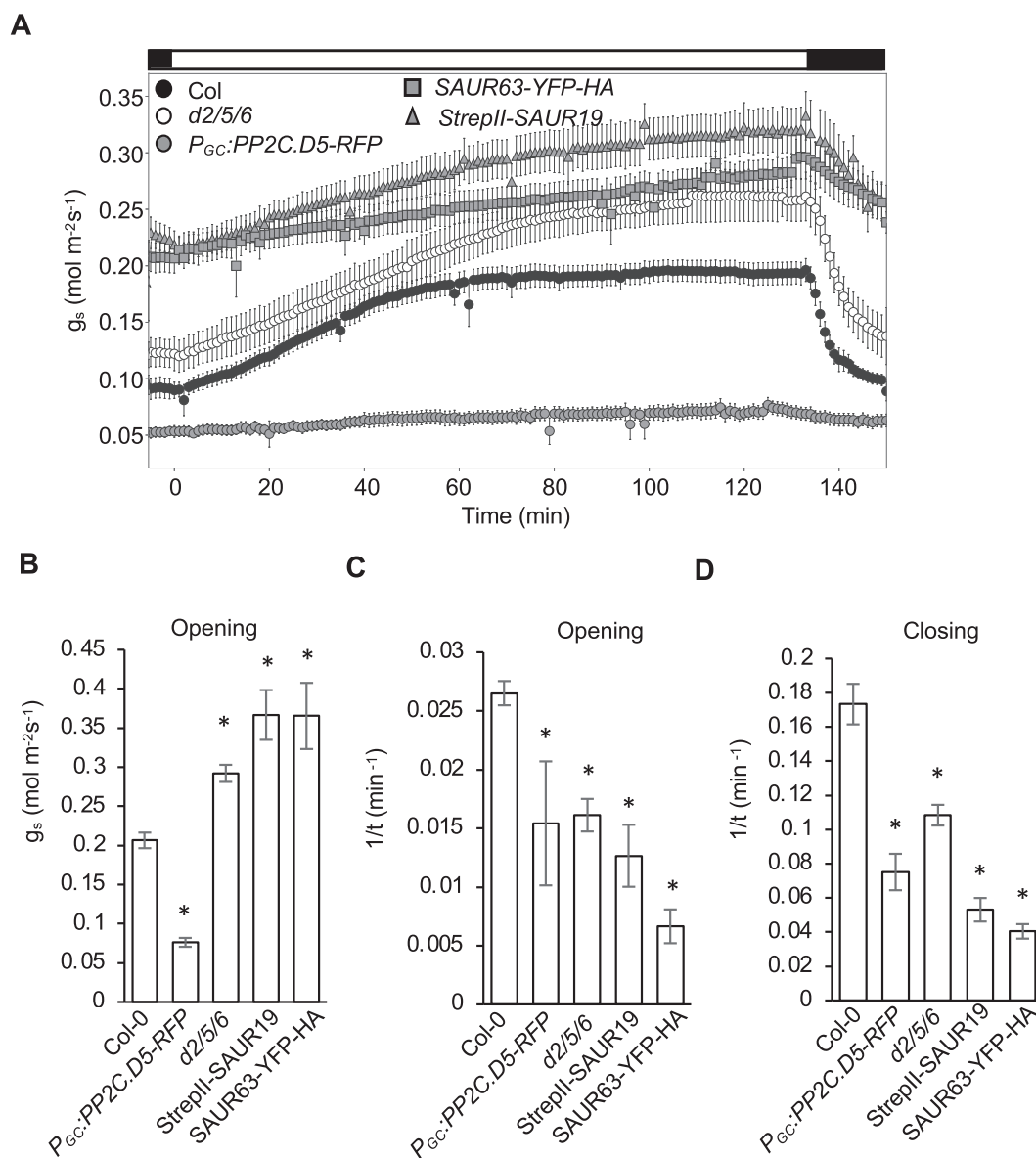


**Figure 3** Gas exchange analyses of *pp2c.d2/5/6* mutant and *SAUR19/63* overexpression plants. (A) Stomatal conductance ( $g_s$ ) response from dark-adapted leaves exposed to light and subsequent transfer back to darkness. Data are means  $\pm$  SE ( $n \geq 5$ ). Bar above figure indicates dark/light/dark transitions. Bar graphs represent (B) maximum stomatal opening, (C)  $b$  value of opening, and (D)  $b$  value of closing. Data are means  $\pm$  SE ( $n \geq 4$ ). Asterisks indicate statistically significant differences relative to wild-type Col-0 determined by one-way analysis of variance Holm test ( $P < 0.05$ ).

in the baseline  $g_s$  in both light and darkness, and were impaired in the dynamic range and kinetics for stomatal movements between the two conditions.

### PP2C.D5 overexpression in guard cells closes stomata constitutively

To explore further the mechanisms by which *PP2C.D2/5/6* promote stomatal closure, we overexpressed *PP2C.D2/5/6-RFP* fusion genes under the control of the guard cell-specific  $P_{GC}$  promoter (Cominelli et al., 2005; Cominelli et al., 2011). Three independent lines of each *PP2C.D2/6-RFP* construct were generated in the wild-type background, and the *PP2C.D5-RFP* construct was introduced into the *pp2c.d5*

single mutant background. Each line was examined by confocal microscopy to confirm guard cell-specific expression (Figure 4, B and Supplemental Figure S5A). Although overexpression of *PP2C.D5* from the 35S promoter or even its native promoter confers severe reductions in plant stature due to its role in regulating cell expansion (Ren et al., 2018), the  $P_{GC}:PP2C.D5-RFP$  transgenic plants displayed no obvious growth defects (Figure 4A). Examination of stomata in these lines, however, showed a modest reduction in guard cell size (Figure 4C). Additionally, using detached leaves we found that all  $P_{GC}:PP2C.D2/5/6-RFP$  transgenic lines exhibited a reduced rate of water loss compared to the wild-type (Figure 4, D and Supplemental Figure S5B).

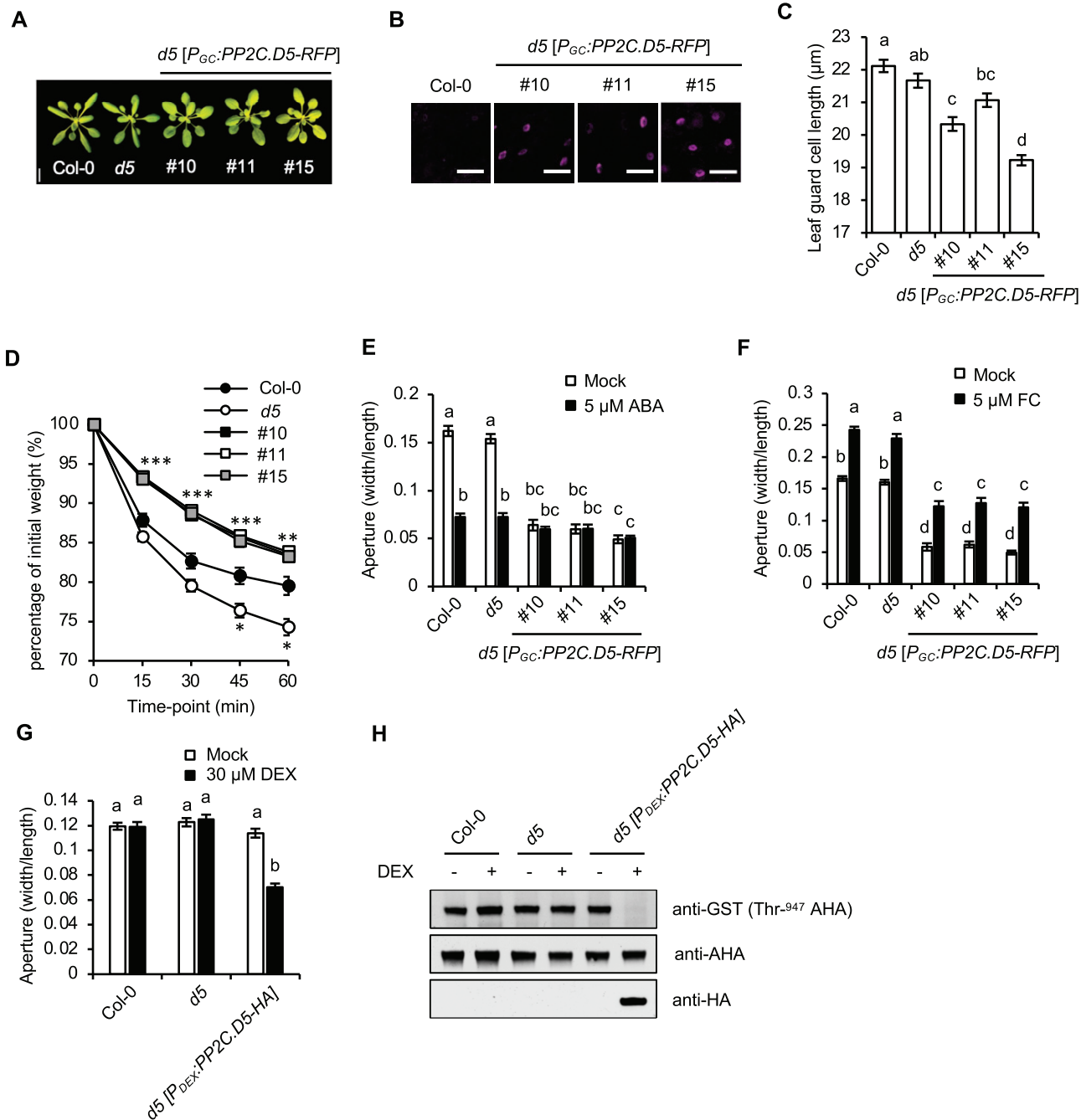


**Figure 4** Overexpression of PP2C.D5 in guard cell confers constitutively closed stomata. **(A)** 24-d-old plants. Three independent *P<sub>Gc</sub>:PP2C.D5-RFP* lines are shown. Scale bar = 1 cm. **(B)** Guard cell-specific expression of *P<sub>Gc</sub>:PP2C.D5-RFP* (magenta) in 14-d-old leaves with wild-type Col-0 as the negative control. Scale bar = 50 µm. **(C)** Stomatal length of leaf guard cells of wild-type Col-0, *pp2c.d5* and *pp2c.d5 [P<sub>Gc</sub>:PP2C.D5-RFP]* plants. Data are means ± SE (*n* = 120). **(D)** Water loss in leaf detachment assays of wild-type Col-0, the *pp2c.d5* single mutant, and *P<sub>Gc</sub>:PP2C.D5-RFP* lines. Data are means ± SE (*n* = 11). Asterisks indicate significant difference from the wild-type (*P* < 0.05, Student's *t* test). The number of asterisks indicate the number of *P<sub>Gc</sub>:PP2C.D5-RFP* lines that differed significantly from wild-type at each time point. **(E)** Stomatal aperture measurements of wild-type Col-0, the *pp2c.d5* single mutant, and *P<sub>Gc</sub>:PP2C.D5-RFP* lines following 2 h mock or 5 µM ABA treatments. Data are means ± SE (*n* = 60). **(F)** Stomatal aperture measurements of wild-type Col-0, the *pp2c.d5* single mutant, and *P<sub>Gc</sub>:PP2C.D5-RFP* lines following 2 h mock or 5 µM FC treatments. Data are means ± SE (*n* = 60). **(G)** Stomatal aperture measurements of wild-type Col-0, the *pp2c.d5* single mutant, and *P<sub>Dex</sub>:PP2C.D5-HA* lines in the absence or presence of 30 µM DEX treatment for 5 h. Data are means ± SE (*n* = 60). **(H)** Examination of AHA Thr-947 phosphorylation in 3-week-old rosette leaves by GST-14-3-3 far-western gel assay. PP2C.D5-HA protein expression levels are shown in the bottom panel. For **(C, E–G)**, different letters above error bars indicate significant difference (*P* < 0.05) by one-way analysis of variance analysis with Tukey's HSD test.



To establish how stomatal behavior is affected by *PP2C.D2/5/6* overexpression, we measured stomatal apertures in epidermal peels of *P<sub>GC</sub>:PP2C.D2/5/6-RFP* leaves under mock and 5  $\mu$ M ABA treatments. All *P<sub>GC</sub>:PP2C.D2/5/6-RFP* lines exhibited constitutively closed stomatal apertures in the light, both in the presence and absence of ABA (Figure 4, E; Supplemental Figure S5C). In agreement with our aperture measurements, gas exchange analysis of *P<sub>GC</sub>:PP2C.D5-RFP* plants indicated a dramatic reduction in  $g_s$ , with only minor opening or closing responses observed in response to light or darkness, respectively (Figure 3, A–D).

To test whether the constitutively closed aperture phenotype of *P<sub>GC</sub>:PP2C.D2/5/6-RFP* plants was related to guard cell size, we examined the apertures of plants expressing dexamethasone (DEX)-inducible *PP2C.D5* fused with an HA tag (*P<sub>Dex</sub>:PP2C.D5-HA*). Uninduced *P<sub>Dex</sub>:PP2C.D5-HA* plants displayed apertures comparable to wild-type controls. However, following a 5-h induction with DEX, *P<sub>Dex</sub>:PP2C.D5-HA* stomata closed (Figure 4G), confirming that *PP2C.D5* promotes stomatal closure.

### Overexpression of *PP2C.D5* represses H<sup>+</sup>-ATPase activity

In expanding cells, *PP2C.D2/5/6* inhibit PM H<sup>+</sup>-ATPase activity by catalyzing dephosphorylation of the penultimate Thr residue in the autoinhibitory domain (corresponding to Thr-947 of AHA2; Ren et al., 2018; Wong et al., 2019). Indeed, penultimate Thr phosphorylation of PM H<sup>+</sup>-ATPases was dramatically diminished in induced *P<sub>Dex</sub>:PP2C.D5-HA* plants (Figure 4H) as shown by GST-14-3-3 far-western blotting assays (Fuglsang et al., 1999; Kinoshita and Shimazaki, 1999; Hayashi et al., 2010). Unfortunately, such biochemical assays of PM H<sup>+</sup>-ATPase phosphorylation status specifically in guard cells are not possible due to high background signal from other cells. We therefore tested whether the closed aperture phenotype of *P<sub>GC</sub>:PP2C.D5-RFP* plants could be rescued by the fungal toxin fusaric acid (FA). FA activates PM H<sup>+</sup>-ATPases by promoting irreversible 14-3-3 protein binding to the C-terminal autoinhibitory domain, preventing dephosphorylation of the penultimate Thr residue (Olsson et al., 1998; Svennelid et al., 1999). FA treatment partially rescued the closed stomatal phenotype (Figure 4F), demonstrating that *P<sub>GC</sub>:PP2C.D5-RFP* stomata can in fact open, and confirming that the constitutively closed phenotype is not due to the effect of *PP2C.D5* overexpression on guard cell size. Importantly, these results suggest that low H<sup>+</sup>-ATPase activity impacts stomatal opening in these plants.

*AHA1* encodes the primary PM H<sup>+</sup>-ATPase responsible for driving stomatal opening, with *AHA2* playing a minor supporting role (Merlot et al., 2007; Wang et al., 2014; Yamauchi et al., 2016). To test genetically whether increased H<sup>+</sup>-ATPase activity could rescue the closed stomata of *P<sub>GC</sub>:PP2C.D5-RFP* plants, we transformed the *P<sub>GC</sub>:PP2C.D5-RFP* construct into the *ost2-2 aha2-5* genetic background, in which the gain-of-function *ost2-2* allele increases *AHA1* activity. Three

independent lines displaying guard cell-specific expression of *PP2C.D5-RFP* were analyzed (Figure 5A). *ost2-2 aha2-5[P<sub>GC</sub>:PP2C.D5-RFP]* plants exhibited phenotypes intermediate between those of *P<sub>GC</sub>:PP2C.D5-RFP* and *ost2-2 aha2-5* plants in both water loss (Figure 5B) and stomatal aperture assays (Figure 5C). Again, these results suggest that H<sup>+</sup>-ATPase activity limits stomatal opening in the *P<sub>GC</sub>:PP2C.D5-RFP* plants. However, as neither FA treatment nor the *ost2-2* mutation could entirely suppress the *P<sub>GC</sub>:PP2C.D5-RFP* stomatal phenotypes, the data raise the possibility that *PP2C.D5* affects other targets in addition to the H<sup>+</sup>-ATPase.

### Guard cell SAURs interact with *PP2C.D* proteins to control stomatal aperture

As described above, *SAUR56* and *SAUR60* expression are highly enriched in guard cells. Furthermore, overexpression of these *SAURs* in guard cells confers a constitutively open stomatal phenotype (Figure 1, H–J) similar to the *pp2c.d2/5/6* triple mutant, suggesting that these *SAURs* may antagonize *PP2C.D* function as has been described for *SAUR19* during organ growth (Spartz et al., 2014, 2017). To test this possibility, we examined the ability of *SAUR56* and *SAUR60* to interact with *PP2C.D* phosphatases. In both yeast two-hybrid and bimolecular fluorescence complementation assays, both *SAUR* proteins interacted with *PP2C.D* proteins (Figure 6, A; Supplemental Figure S6). Moreover, in *in vitro* phosphatase assays, recombinant *SAUR56* or *SAUR60* proteins inhibited *PP2C.D*-mediated dephosphorylation of Thr-947 of *AHA2* (Figure 6B). Together, these findings suggest that *SAUR56* and *SAUR60* may inhibit *PP2C.D* phosphatases to promote PM H<sup>+</sup>-ATPase activity specifically in guard cells.

To explore further the roles of *SAUR56* and *SAUR60* in stomatal physiology, we used CRISPR/Cas9-mediated genome editing to make frameshift mutations in the genomic coding sequences of both genes (Supplemental Figure S7A), and crossed these lines to obtain double mutants among the progeny. Two lines containing independent mutations in both *SAUR* genes were obtained (*saur56-1 saur60-2* and *saur56-2 saur60-1*). In stomatal aperture assays, these double mutants displayed decreased apertures compared to the wild-type in the light (Figure 7, A; Supplemental Figure S7B). Consistent with this finding, *saur56-1 saur60-2* plants exhibited reduced  $g_s$  in the light, as did the corresponding single mutants, albeit to a lesser extent (Figure 7, B and C). Moreover, a genomic *SAUR56* transgene rescued the reduced stomatal aperture phenotype of *saur56-1 saur60-2* double mutant plants partially or fully, depending on the transformant (Supplemental Figure S7D). Taken together, the results indicate that *SAUR56* and *SAUR60* act partially redundantly to open stomata in the light.

Given that *SAUR56* and *SAUR60* can inhibit *PP2C.D* phosphatase activity, we hypothesized that the *saur56/60* mutant phenotypes would be dependent upon *PP2C.D* function. To examine genetic interactions between these *SAUR* and *PP2C.D* proteins, we measured stomatal apertures of *pp2c.d2/*



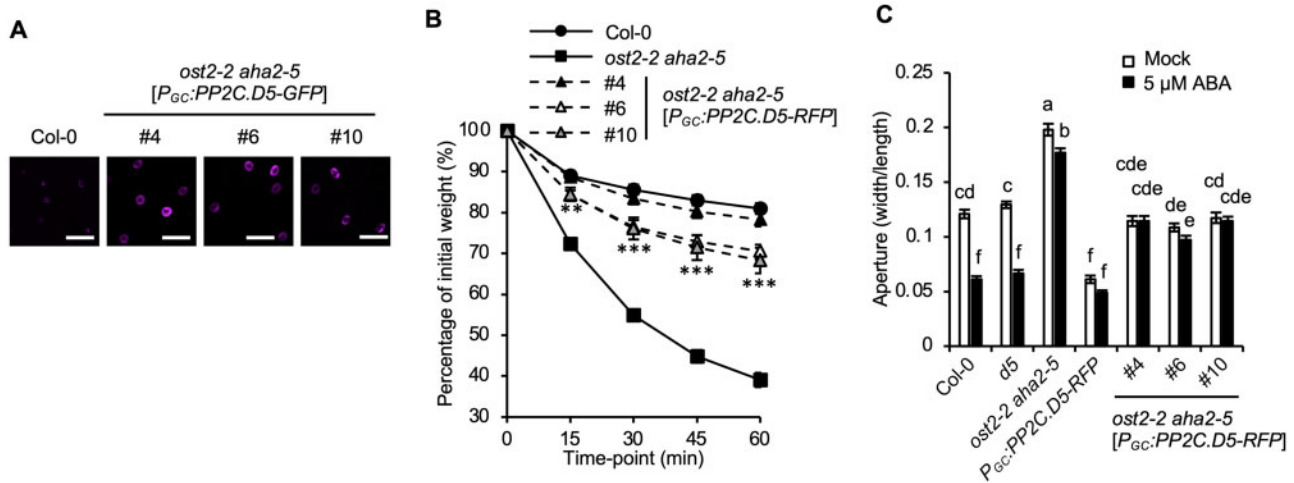


**Figure 5** The *ost2-2* mutation partially suppresses the PGC:PP2C.D5-RFP closed stomata phenotype. **(A)** Guard cell-specific expression of PP2C.D5-RFP (magenta) in 14-d-old leaves of *ost2-2 aha2-5* mutants with wild-type Col-0 as a negative control. Scale bar = 50  $\mu$ m. **(B)** Water loss in leaf detachment assays of wild-type Col-0, the *ost2-2 aha2-5* double mutant, and *ost2-2 aha2-5*[P<sub>GC</sub>:PP2C.D5-RFP] plants. Data are means  $\pm$  SE ( $n = 12$ ). Asterisks indicate significant difference from the *ost2-2 aha2-5* parental line ( $P < 0.05$ , Student's  $t$  test). The number of asterisks indicate the number of P<sub>GC</sub>:PP2C.D5-RFP lines that differed significantly from *ost2-2 aha2-5* at each time point. **(C)** Stomatal aperture measurements of wild-type Col-0, *pp2c.d5* single mutant, *ost2-2 aha2-5* double mutant, and P<sub>GC</sub>:PP2C.D5-RFP in either the *pp2c.d5* or *ost2-2 aha2-5* genetic backgrounds following 2 h mock or 5  $\mu$ M ABA treatments. Data are means  $\pm$  SE ( $n = 60$ ). Different letters above error bars indicate significant difference ( $P < 0.05$ ) by one-way analysis of variance analysis with Tukey's HSD test.

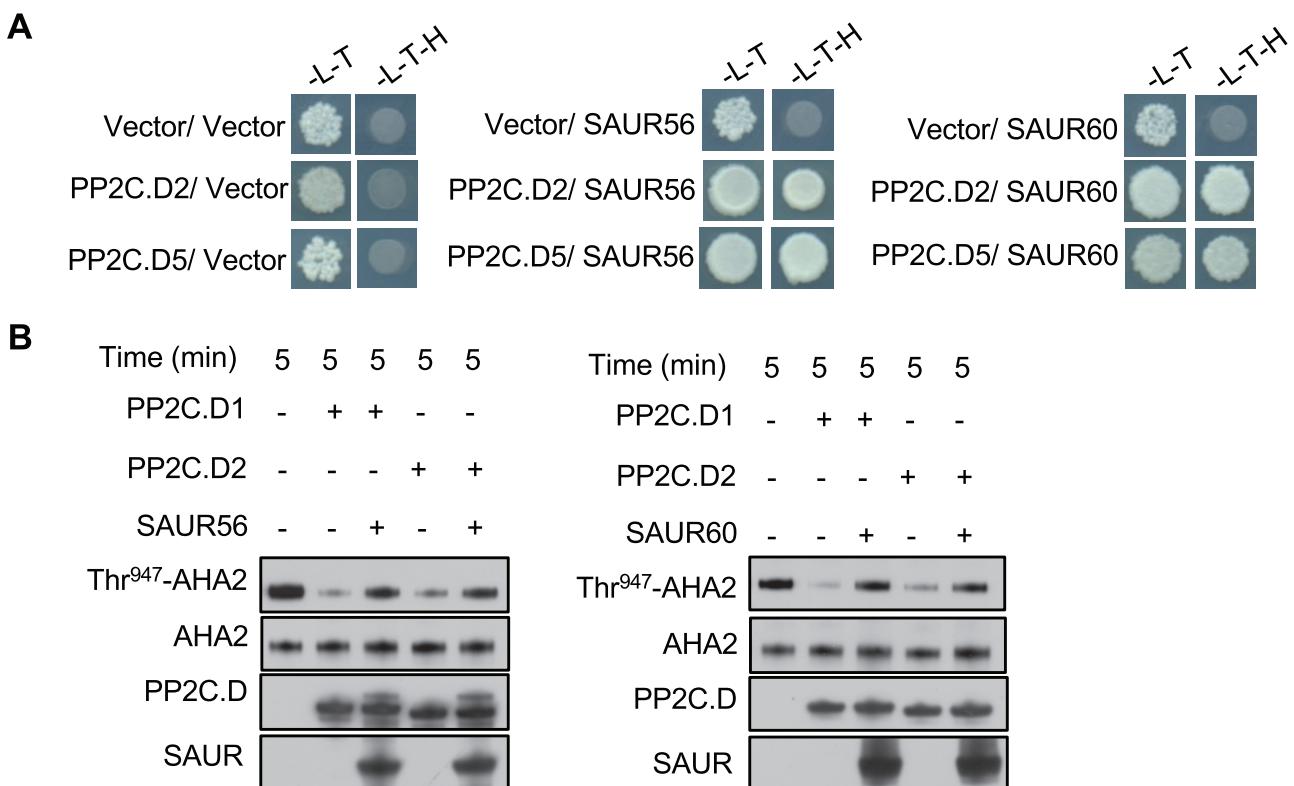


**Figure 6** SAUR56 and SAUR60 repress PP2C.C phosphatase activity. **(A)** Interaction between SAUR56/SAUR60 and PP2C.D phosphatases in yeast two-hybrid assays. Diluted yeast cultures were spotted onto Leu, Trp (-L-T) or Leu, Trp, His (-L-T-H) dropout plates and incubated for 3–4 d. **(B)** In vitro phosphatase assays employing yeast-expressed AHA2. Recombinant SAUR56 (left) and SAUR60 (right) inhibit PP2C.D-mediated dephosphorylation of Thr-947 of AHA2. Thr-947 phosphorylation status was assessed by GST-14-3-3 far-western blotting, and PP2C.D1/2 and SAUR56/60 abundance was monitored by detection of the S-tag.

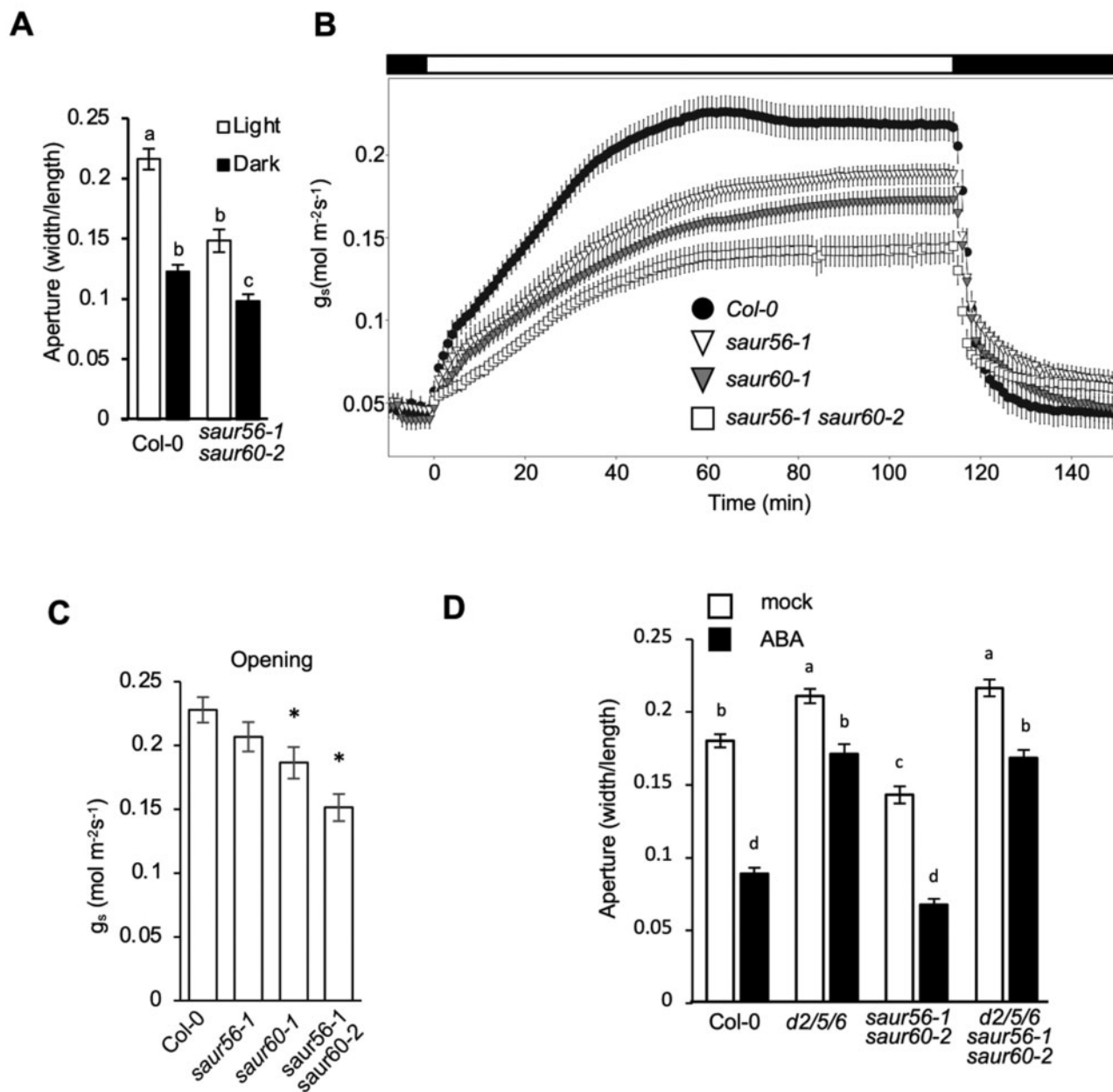


**Figure 7** SAUR56 and SAUR60 regulate stomatal aperture. (A) Stomatal aperture measurements of wild-type and *saur56-1 saur60-2* mutant plants under light and dark conditions. Data are means  $\pm$  SE ( $n \geq 80$ ). (B) Stomatal conductance ( $g_s$ ) response from dark-adapted plants exposed to light and subsequent transfer back to darkness. Data are means  $\pm$  SE ( $n \geq 7$ ). Bar above figure indicates dark/light/dark transitions. (C) Maximum stomatal opening obtained in  $g_s$  assays. Data are means  $\pm$  SE ( $n \geq 7$ ). Asterisks indicate statistically significant differences relative to wild-type Col-0 determined by one-way analysis of variance Holm test ( $P < 0.05$ ). (D) Stomatal aperture measurements following a 2 h treatment with 5  $\mu$ M ABA or solvent control. Data are means  $\pm$  SE ( $n \geq 65$ ). For (A and D), different letters above error bars indicate significant difference ( $P < 0.05$ ) by one-way analysis of variance analysis with Tukey's HSD test.

5/6 *saur56/60* quintuple mutants. The *pp2c.d2/5/6* mutations were largely epistatic to *saur56/60*, with the quintuple mutant stomata displaying a nearly identical increased aperture phenotype as seen with *pp2c.d2/5/6* stomata in both the absence and presence of ABA (Figure 7D). Excised leaves of *pp2c.d2/5/6 saur56/60* quintuple mutant plants also lost water at a rate comparable to the *pp2c.d2/5/6* triple mutant (Supplemental Figure S7C). These results suggest that SAUR56 and SAUR60

require the PP2C.D proteins for their action, consistent with the ability of these SAUR proteins to inhibit PP2C.D activity.

### SAURs and PP2C.D2/5/6 regulate K<sup>+</sup> channel activities in guard cells

Our findings that FC treatment or the *ost2-2* mutation each only partially suppressed stomatal closure in the *P<sub>GC</sub>:PP2C.D5-RFP* plants suggest that PP2C.D phosphatases

may have additional targets beside  $H^+$ -ATPases in the regulation of stomatal movements. To explore this question in detail, we carried out voltage clamp analyses to quantify the dominant  $K^+$  channel activities in the guard cells. After instantaneous background current subtraction, steady-state currents were fitted to a Boltzmann function of the following form:

$$I_K = g_{\max} * (V - E_K) / (1 + e^{\delta F (V - V_{1/2}) / RT}) \quad (3)$$

where  $V_{1/2}$  is the voltage giving half-maximal activation of the current  $I_K$ ,  $\delta$  is the voltage sensitivity coefficient,  $g_{\max}$  is the maximum conductance,  $E_K$  is the  $K^+$ -equilibrium voltage, and  $R$  and  $T$  have their usual meanings.

We first examined the inward- ( $I_{K,in}$ ) and outward-rectifying ( $I_{K,out}$ )  $K^+$  channel activities in the *pp2c.d2/5/6* mutant and gain-of-function *P<sub>GC</sub>:PP2C.D5-RFP* lines. Fittings for each current yielded a common set of voltage-sensitivity coefficients ( $\delta$ ; Figure 8, A and Table 1, top), consistent with the previous analyses of the channels (Hosy et al., 2003; Wang et al., 2012, 2017; Jezek and Blatt, 2017). Additionally,  $I_{K,in}$  data were fitted with a common  $V_{1/2}$ , much as reported in the past (Wang et al., 2012; Jezek and Blatt, 2017; Lefoulon et al., 2018).

Analysis of the *pp2c.d2/5/6* mutant showed, for  $I_{K,out}$ , a small increase in  $g_{\max}$  and a highly significant shift in  $V_{1/2}$  to more negative voltages (Figure 8, A and Table 1, top), whereas the opposite was observed in the *P<sub>GC</sub>:PP2C.D5-RFP* transgenic guard cells, which exhibited reduced  $g_{\max}$  and a significant shift in  $V_{1/2}$  to more positive voltages relative to the wild-type (Figure 8, A and Table 1, top). A complementary pattern in response was observed for  $I_{K,in}$ . In this case, the current in the *pp2c.d2/5/6* mutant was greatly reduced, whereas in the *P<sub>GC</sub>:PP2C.D5-RFP* guard cells it was enhanced when compared with wild-type guard cells (Figure 8, A and Table 1, top). Thus, loss and gain of *PP2C.D2/5/6* function in the guard cells led to reciprocal changes in the  $K^+$  channel activities, the effect being opposite between the two currents. Significantly, the effects on  $I_{K,out}$  were not restricted to scalar changes in the ensemble conductance  $g_{\max}$ , but also affected the mid-point voltage,  $V_{1/2}$ , for gating. Such an effect cannot be explained on the basis of a change in the population of channels and implies a direct effect on the gating process itself (Jezek and Blatt, 2017). Thus, our findings suggest that these phosphatases positively regulate the inward-rectifying channels and affect the voltage-dependence of gating of the outward-rectifying  $K^+$  channels.

We also analyzed the  $K^+$  channel currents recorded from *SAUR19/63* overexpression lines and *saur56/60* mutants. Recordings of  $I_{K,out}$  in both *SAUR* overexpression lines showed characteristics similar to those of the *pp2c.d2/5/6* triple mutant, with a negative shift in  $V_{1/2}$  compared with wild-type guard cells (Supplemental Figure S8 and Table 1, top). However,  $g_{\max}$  values for  $I_{K,out}$  in the *SAUR19/63* overexpressing lines were only half that of the *pp2c.d2/5/6* mutant and the wild-type. In contrast, the *saur56 saur60* double mutant exhibited increased  $I_{K,out}$  conductance in

comparison with wild-type guard cells and a highly significant positive shift in  $V_{1/2}$  relative to the wild-type (Figure 8, B and Table 1, bottom). In both *SAUR* overexpression lines, values for  $g_{\max}$  of  $I_{K,in}$  were much lower than in the wild-type and slightly lower than the *pp2c.d2/5/6* knockout mutants (Supplemental Figure S8 and Table 1, top). Conversely, for the *saur56 saur60* guard cells,  $g_{\max}$  of this current was enhanced by more than three-fold in comparison with the wild-type (Figure 8, B and Table 1, bottom). Thus, we conclude that, in general, the *SAURs* reduce  $I_{K,in}$  ensemble activity, plausibly through a reduction in the population of activatable channels. Together, these findings suggest that *SAUR* and *PP2C.D* proteins have largely opposing effects on inward-rectifying and outward-rectifying  $K^+$  channel conductances. Their effects on the outward-rectifying  $K^+$  channel are more complex and include significant effects on gating as indicated by the effects on  $V_{1/2}$ .

## Discussion

### Regulation of stomatal aperture by *SAUR* and *PP2C.D* proteins

Our results using both gain- and loss-of-function plants indicate that *SAUR* and *PP2C.D* proteins act antagonistically to regulate stomatal aperture. In aperture assays, we demonstrated that overexpression of *SAUR19*, *SAUR63*, *SAUR56*, or *SAUR60* fusion proteins all resulted in increased apertures under multiple conditions. Of these, *SAUR56* and *SAUR60* are expressed in guard cells and normally regulate stomatal aperture, whereas *SAUR19* and *SAUR63* are not expressed in guard cells and instead normally regulate cell expansion in growing tissues (Chae et al., 2012; Spartz et al., 2012). Likewise, the *SAUR*-regulated *PP2C.D2*, *PP2C.D5*, and *PP2C.D6* phosphatases are also expressed in guard cells, and loss-of-function *pp2c.d2/5/6* mutants exhibit increased stomatal apertures. Reciprocally, gain-of-function *PP2C.D5* lines and loss-of-function *saur56/60* mutants display reductions in stomatal aperture. These findings are further supported by results obtained in stomatal conductance and water loss assays and are consistent with *SAUR* proteins inhibiting *PP2C.D* phosphatase function to control stomatal aperture. Moreover, the *SAUR56* and *SAUR60* proteins, which are expressed in guard cells, can interact with the *PP2C.D2/5/6* phosphatases and inhibit their enzymatic activity. Together, these findings implicate *SAUR*–*PP2C.D* regulatory modules in stomatal aperture control, with *SAURs* inhibiting *PP2C.D2/5/6* activity to promote stomatal opening.

During organ growth, auxin-induced *SAUR* proteins inhibit *PP2C.D2/5/6*-mediated dephosphorylation of the penultimate Thr residue within the autoinhibitory domain of *PM H<sup>+</sup>-ATPases*, resulting in cell expansion via an acid growth mechanism (Spartz et al., 2014; Ren et al., 2018; Wong et al., 2019; Du et al., 2020). Given the well-established role of  $H^+$  *ATPases* in driving stomatal opening (Kinoshita and Shimazaki, 1999; Inoue and Kinoshita, 2017; Ando and Kinoshita, 2018), it seems likely that guard cell *SAURs*, including *SAUR56* and *SAUR60*, may similarly activate  $H^+$ -

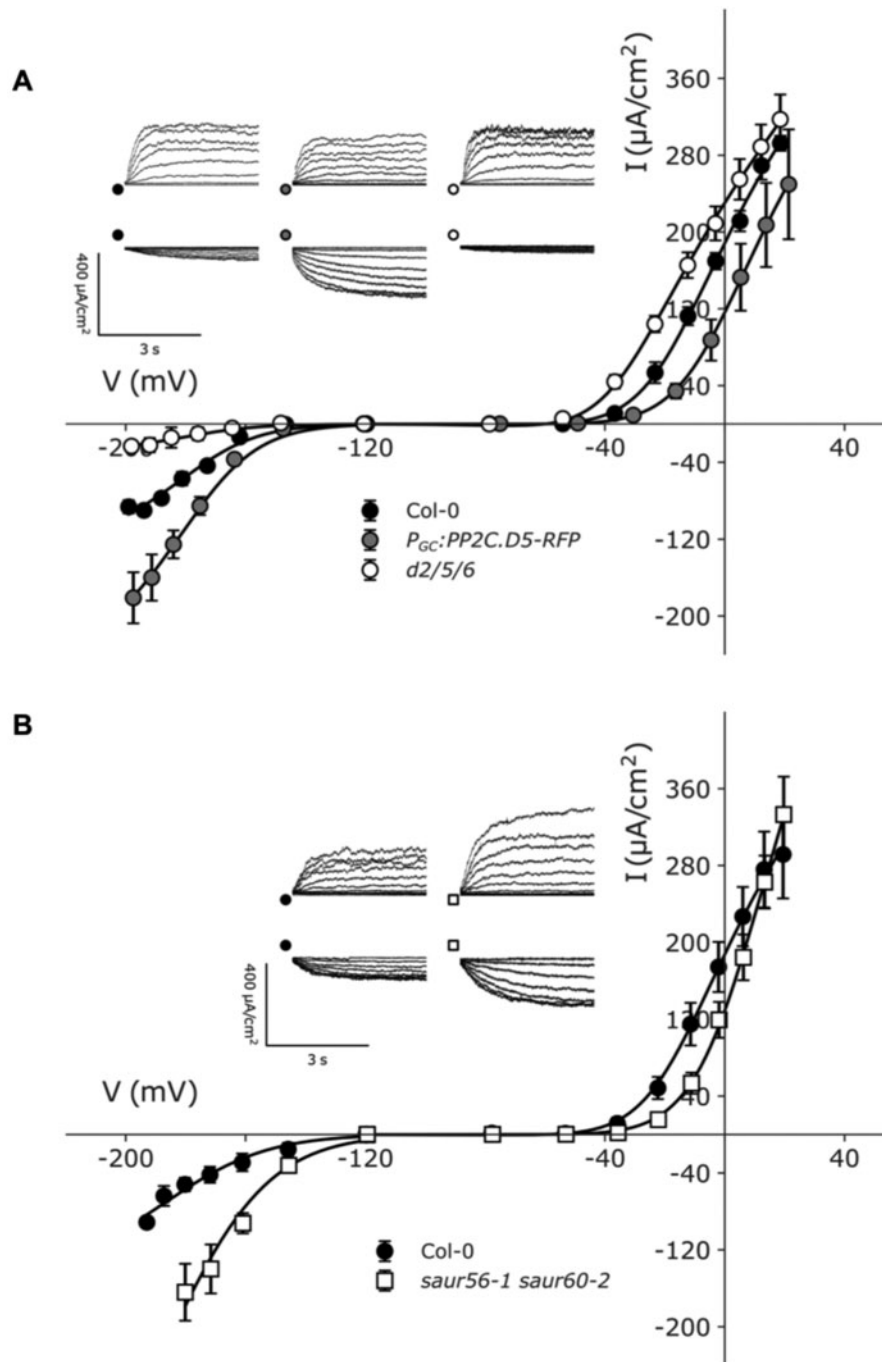


**Figure 8** Characteristics of  $K^+$ -out and  $K^+$ -in channels in guard cells of plants with altered SAUR–PP2C.D function. Voltage clamp measurements of guard cells of wild-type Col-0, *pp2c.d2/5/6* triple mutant, *P<sub>GC</sub>:PP2C.D5-RFP* and *saur56-1 saur60-2* double mutant. Voltage stepped from a holding potential of  $-120$  to  $+20$  mV for  $I_{K,out}$  and from  $-120$  to  $-210$  mV for  $I_{K,in}$ . Data are means  $\pm$  SE ( $n \geq 4$ ) for each dataset. Fittings were performed jointly for each current. Scale:  $400 \mu A/cm^2$  vertical,  $3$  s horizontal. (A) *P<sub>GC</sub>:PP2C.D5-RFP*  $K^+$  channel data are plotted together with *pp2c.d2/5/6* mutant and wild-type Col-0. Fittings for  $I_{K,out}$  yielded common voltage-sensitivity coefficients ( $\delta$ ) of  $-2.12 \pm 0.08$ . The data for  $I_{K,in}$  were fitted with common voltage-sensitivity coefficients ( $\delta$ )  $-1.47 \pm 0.21$  and the common midpoint voltage ( $V_{1/2}$ ) for  $I_{K,in}$   $-176 \pm 2$  mV. (B) *saur56-1 saur60-2* data are plotted together with wild-type Col-0. Fittings for  $I_{K,out}$  yielded common voltage-sensitivity coefficients ( $\delta$ ) of  $2.12 \pm 0.15$ . The data for  $I_{K,in}$  were fitted with common voltage-sensitivity coefficients ( $\delta$ )  $-1.40 \pm 0.24$  and the common midpoint voltage ( $V_{1/2}$ ) for  $I_{K,in}$   $-179 \pm 8$  mV.

ATPases by inhibiting PP2C.D function to regulate stomatal aperture. The similar aperture behaviors of SAUR overexpressors, *pp2c.d2/5/6* mutants and the *ost2-2* gain-of-function allele of the AHA1 PM  $H^+$ -ATPase support this

hypothesis. Furthermore, the finding that the *pp2c.d2/5/6* open stomate phenotype is epistatic to the reduced aperture phenotype of *saur56/60* mutants strongly suggests that these SAURs work through the PP2C.D2/5/6



**Table 1** Steady-state currents of wild-type, *pp2c.d2/5/6* triple mutant, *PP2C.D5* and *SAUR19/63* overexpression lines and *saur56-1 saur60-2* double mutant fitted to a Boltzmann function

| Genotype                      | $g_{\max}$ (mS cm <sup>-2</sup> ) | $V_{1/2}$ (mV)         | $\delta$     |
|-------------------------------|-----------------------------------|------------------------|--------------|
| <i>I<sub>K,out</sub></i>      |                                   |                        |              |
| Col 0                         | 3.93 ± 0.05 <sup>(A)</sup>        | -16 ± 1 <sup>(X)</sup> | 2.12 ± 0.08  |
| <i>pp2c.d2/5/6</i>            | 4.07 ± 0.03 <sup>(A)</sup>        | -33 ± 1 <sup>(Y)</sup> |              |
| <i>P<sub>CC</sub>:PP2C.D5</i> | 3.49 ± 0.0 <sup>(B)</sup>         | -3 ± 1 <sup>(Z)</sup>  |              |
| <i>StrepII-SAUR19</i>         | 1.81 ± 0.03 <sup>(C)</sup>        | -31 ± 2 <sup>(Y)</sup> |              |
| <i>SAUR63-YFP-HA</i>          | 1.98 ± 0.02 <sup>(C)</sup>        | -42 ± 3 <sup>(Y)</sup> |              |
| <i>I<sub>K,in</sub></i>       |                                   |                        |              |
| Col-0                         | 0.79 ± 0.06 <sup>(a)</sup>        | -176 ± 2               | -1.47 ± 0.21 |
| <i>pp2c.d2/5/6</i>            | 0.19 ± 0.03 <sup>(b)</sup>        |                        |              |
| <i>P<sub>CC</sub>:PP2C.D5</i> | 1.55 ± 0.10 <sup>(c)</sup>        |                        |              |
| <i>StrepII-SAUR19</i>         | 0.14 ± 0.03 <sup>(b)</sup>        |                        |              |
| <i>SAUR63-YFP-HA</i>          | 0.00 ± 0.03 <sup>(d)</sup>        |                        |              |
| <i>I<sub>K,out</sub></i>      |                                   |                        |              |
| Col-0                         | 3.98 ± 0.10 <sup>(1)</sup>        | -15 ± 2 <sup>(x)</sup> | 2.12 ± 0.15  |
| <i>saur56-1 saur60-2</i>      | 5.33 ± 0.33 <sup>(1)</sup>        | 5 ± 2 <sup>(y)</sup>   |              |
| <i>I<sub>K,in</sub></i>       |                                   |                        |              |
| Col-0                         | 0.91 ± 0.19 <sup>(i)</sup>        | -179 ± 8               | -1.40 ± 0.24 |
| <i>saur56-1 saur60-2</i>      | 2.86 ± 0.62 <sup>(i)</sup>        |                        |              |

After instantaneous background current subtraction, steady-state currents were fitted to a Boltzmann function of the form  $I_K = g_{\max} * (V - E_K) / (1 + e^{\frac{\delta F (V - V_{1/2})}{RT}})$ , where  $V_{1/2}$  is the voltage giving half-maximal activation of the current  $I_K$ ,  $\delta$  is the voltage sensitivity coefficient,  $g_{\max}$  is the maximum conductance,  $E_K$  is the K<sup>+</sup> equilibrium voltage, and R and T have their usual meanings. The data were adjusted to ensure the equivalents between Col-0 currents. Fittings for  $I_{K,out}$  yielded common voltage-sensitivity coefficients ( $\delta$ ), and  $I_{K,in}$  were fitted with common voltage-sensitivity coefficients ( $\delta$ ) and common midpoint voltage ( $V_{1/2}$ ). Different letters within each dataset indicate statistically significant differences determined by one-way analysis of variance Scheffe test ( $P < 0.05$ ).

phosphatases. Consistent with this notion, we demonstrated that SAUR56 and SAUR60 inhibit PP2C.D-mediated dephosphorylation of the penultimate Thr residue of H<sup>+</sup>-ATPases in vitro. Direct measurements of H<sup>+</sup>-ATPase activity and phosphorylation specifically in guard cells would be needed to confirm this possibility. However, our data also clearly demonstrate that the SAUR–PP2C.D actions are more complex than this. In short, the effects on the H<sup>+</sup>-ATPase are not sufficient to fully explain the physiological consequences for the guard cell.

Our findings suggest that SAUR56/60-PP2C.D2/5/6 regulatory modules function in guard cells to control stomatal aperture. Notably however, the stomatal opening defect of *saur56/60* double mutants was considerably weaker than that observed for *P<sub>CC</sub>:PP2C.D5-RFP* plants. Likewise, *pp2c.d2/5/6* gas exchange phenotypes were noticeably weaker than those elicited by SAUR overexpression lines. These differences are likely due, at least in part, to additional functional redundancy within the SAUR and PP2C.D gene families. Several other SAUR genes are expressed in guard cells (Supplemental Figure S2A; Bauer et al., 2013; Adrian et al., 2015) and may act together with SAUR56 and SAUR60 to inhibit PP2C.D proteins and promote stomatal opening. Similarly, several additional PP2C.D family members are expressed in guard cells (Supplemental Figure S3), have been previously reported to bind SAUR proteins (Sun et al., 2016;

Ren et al., 2018), and therefore may contribute to stomatal aperture control.

Arabidopsis has nine PP2C.D genes, at least three of which, PP2C.D2, PP2C.D5, and PP2C.D6, plays important roles both in regulating cell expansion during organ growth and in stomatal aperture control. In contrast, Arabidopsis has 79 SAUR genes. Many of these are induced by growth hormones and expressed in growing portions of the plant (Ren and Gray, 2015), whereas a distinct set of SAUR genes, including SAUR56 and SAUR60 are expressed in guard cells (Yang et al., 2008; Wang et al., 2011; Bauer et al., 2013). It thus appears that over evolutionary time, SAUR genes have diversified to acquire cell type-specific functions, at least in part by engaging the PP2C.D-H<sup>+</sup>-ATPase cellular machinery that is present in nearly all plant cells. It seems plausible that, in parallel to SAUR genes acquiring cell type-specific gene expression, SAUR proteins may also have diversified in their quantitative biochemical or regulatory properties.

### Effects on K<sup>+</sup> currents

PM H<sup>+</sup>-ATPase activation by either FC or the *ost2-2* allele was able to suppress the closed stomata phenotype of *P<sub>CC</sub>:PP2C.D5-RFP* plants only partially. This raises the possibility that SAUR–PP2C.D modules may regulate additional targets that contribute to guard cell dynamics. The demonstrable effects of SAUR and PP2C.D expression we identify for K<sup>+</sup> channels strongly support this possibility. Indeed, our detailed knowledge of guard cell membrane transport shows that the concerted action on several transporters during stomatal movements is the norm rather than the exception (Jezek and Blatt, 2017).

The *pp2c.d2/5/6* mutant, as well as *SAUR19/63* overexpressors, each exhibited dramatic reductions in inward-rectifying K<sup>+</sup> channel activity. These results are similar to previous findings with the *ost2-2* mutant, which also exhibited reduced  $I_{K,in}$  currents, reportedly as a consequence of elevated  $[Ca^{2+}]_i$  and  $pH_i$  (Wang et al., 2017). Conversely, the *P<sub>CC</sub>:PP2C.D5-RFP* and *saur56 saur60* guard cells showed increased activity of the inward-rectifying K<sup>+</sup> current. In each case, SAUR and PP2C.D proteins appear to affect this K<sup>+</sup> current antagonistically and in a manner consistent with their predicted effects on H<sup>+</sup>-ATPase activity (Wang et al., 2017). The effects on stomatal aperture and kinetics, however, defy naive expectations with these changes in current. Such counterintuitive associations are typical for a system of transporters in which the activities of several system components interact in nonlinear fashion across a common membrane. That an increase in the inward-rectifying K<sup>+</sup> current accompanied a decrease in stomatal opening, thus highlighting the mechanistic complexity of solute transport that drives stomatal physiology.

Changes in SAUR and PP2C.D activity also affected the outward-rectifying K<sup>+</sup> channels, but in this case, not in a manner that could be explained through a simple SAUR–PP2C.D antagonism. Although both *ost2-2* (Wang et al., 2017) and *pp2c.d2/5/6* mutants exhibited increased activity of the outward-rectifying K<sup>+</sup> channels, as evident in the

$g_{\max}$  unlike *ost2-2*, the *pp2c.d2/5/6* mutants also showed a shift in  $V_{1/2}$  to the left along the voltage axis. Consistent with these findings, *PP2C.D5* overexpression conferred reciprocal effects on  $g_{\max}$  and  $V_{1/2}$ . In contrast, the *SAUR19* and *SAUR63* overexpression lines displayed reductions in  $g_{\max}$  for  $I_{K_{\text{out}}}$  and displaced  $V_{1/2}$  to the left along the voltage axis, whereas the *saur56/60* plants showed an increase in  $g_{\max}$  and displaced  $V_{1/2}$  to the right along the voltage axis. Thus, the effect on  $V_{1/2}$  of the *pp2c.d2/5/6* mutant was similar to that of the *SAUR19* and *SAUR63* overexpression lines, but the two sets of data differed in the consequences for  $g_{\max}$ . To our knowledge, such disparate effects of *SAUR* overexpression and *pp2c.d2/5/6* mutation have not been observed before, and the finding points to *SAUR* regulation of the outward-rectifying  $K^+$  channels that is independent of the *PP2C.D2/5/6* phosphatases. Curiously, while *SAUR* overexpression and *pp2c.d2/5/6* mutation had opposing effects on outward-rectifying  $K^+$  channel activity, both perturbations similarly altered voltage-dependent gating, shifting  $V_{1/2}$  toward more negative voltages than observed in wild-type guard cells. Conversely, the *saur56 saur60* mutant and  $P_{GC}:PP2C.D5-RFP$  guard cells had a more positive  $V_{1/2}$  threshold. These findings may suggest that *SAUR* proteins regulate multiple aspects of outward-rectifying  $K^+$  channel activity, some of which are dependent upon *PP2C.D2/5/6* (i.e. voltage gating) and others that are not. Such regulation could occur via other *PP2C.D* family members or as yet to-be-discovered *SAUR* targets. Importantly, the effects of *SAUR* and *PP2C.D* perturbation on the outward-rectifying  $K^+$  channels do not match any effects previously associated with  $H^+$ -ATPase superactivity, as reflected in the *ost2* mutants (Wang et al., 2017), and therefore cannot be ascribed solely to an effect of elevated  $H^+$ -ATPase activity, such as a rise in pH. One intriguing possibility is that *SAUR*–*PP2C.D* regulatory modules control the phosphorylation status of  $K^+$  channels or regulators thereof to alter channel regulatory properties.

## Conclusion

Our findings provide evidence that *SAUR*–*PP2C.D* regulatory modules control stomatal movements, demonstrating that a common regulatory mechanism controls cell expansion during organ growth and reversible guard cell movements. We also demonstrate that *SAUR* and *PP2C.D* proteins affect not just the PM  $H^+$ -ATPase but also the activities of two different guard cell  $K^+$  channels. The identification of additional *SAUR/PP2C.D* regulatory targets and studies examining mechanisms of effects on  $K^+$  channels are promising areas for future research aimed at elucidating the regulation of stomatal opening and closing dynamics.

## Materials and methods

### Plant materials and growth conditions

All *Arabidopsis* (*Arabidopsis thaliana*) lines used in this article were in the Col-0 ecotype. Seeds were sterilized using 30% (v/v) bleach and 0.04% (v/v) Triton X-100 for 15 min,

and then washed three times with sterile water. The sterilized seeds were grown on ATS media at 22°C after 3 d of stratification. Generation of transgenic plants was done by the floral dip method using *Agrobacterium tumefaciens* strain GV3101 (helper plasmid pMP90) harboring the binary vector with desired target genes (Clough and Bent, 1998). The *GFP-SAUR19* and *StreptII-SAUR19* transgenic lines have been described previously (Spartz et al., 2012).

### Molecular cloning

Primers used for all cloning steps and genotyping assays are listed in Supplemental Table S1. For the guard cell promoter-driven *PP2C.D* ( $P_{GC}:PP2C.D-RFP$ ) and *SAUR* constructs, a full-length *PP2C.D2* cDNA lacking a stop codon, or genomic fragments of *PP2C.D5* and *PP2C.D6* flanking the start codon and last amino acid, were cloned into pENTR/D-TOPO entry vector (Life Technologies). *SAUR56* and *SAUR60* open reading frames were similarly cloned into pENTR/D-TOPO. The entry clones harboring respective genes were recombined into V400/W008 destination vector containing an ABA-insensitive derivative of the guard cell-specific *MYB60* promoter using Gateway LR clonase II enzyme mix (Life Technologies; Karimi et al., 2002).

For the  $35S:SAUR63-YFP-HA$  construct, the full-length *SAUR63* coding sequence without a stop codon was cloned into pENTR/D-TOPO entry clone. The entry clone harboring *SAUR63* cDNA was recombined into destination vector pEarleyGate101 containing YFP and HA tags, pMDC140 containing GUS (Curtis and Grossniklaus, 2003), or a pMDC7 derivative vector containing an estradiol induction system and C-terminal CerFP-HA fusion protein using Gateway LR clonase II enzyme (Earley et al., 2006; Akimoto-Tomiya et al., 2012).

For the  $P_{SAUR56}:SAUR56-GUS$  construct, a fragment incorporating ~1 kb directly upstream of the start codon and the *SAUR56* coding sequence lacking a stop codon was amplified by PCR. For  $P_{SAUR60}:GUS$ , only the upstream 1 kb region was amplified. These PCR products were cloned into pENTR/D-TOPO entry vector (Life Technologies), verified by sequencing, and recombined into destination vector pGWB3 containing a GUS reporter tag using Gateway LR clonase II enzyme (Life Technologies; Nakagawa et al., 2007).

For the  $P_{SAUR56}:SAUR56$  complementation construct, a fragment incorporating ~1 kb directly upstream of the start codon, the *SAUR56* coding sequence, and ~500 bp downstream from the stop codon was amplified by PCR. This product was cloned into pENTR/D-TOPO entry vector (Life Technologies), verified by sequencing, and recombined into destination vector pGWB1 using Gateway LR clonase II enzyme (Life Technologies; Nakagawa et al., 2007). This construct was introduced into *saur56-1 saur60-2* double knockout plants via floral dip for isolation of transgenic lines.

For CRISPR/Cas9 targeting of *SAUR56* and *SAUR60*, single guide RNAs targeting *SAUR56* or *SAUR60* were cloned by SLIM tailed PCR (Chiu et al., 2004) into pDONR207 vector (Life Technologies), subcloned into destination binary vector

pCUT6 (Peterson et al., 2016) by LR clonase (Invitrogen), and introduced into *Arabidopsis* ecotype Columbia plants by floral dip (Clough and Bent, 1998) using *A. tumefaciens* strain GV3101 pMP90. Basta-resistant T1 transformed plants were selected on soil by spraying with 0.01% (v/v) Finale (Bayer Environmental Science, RTP, NC, USA). Mutations were identified in the T2 generation by detecting size differences on 15% (w/v) polyacrylamide gels of PCR products spanning the target sites, and by sequencing PCR products spanning the targeted sites.

### GCPs isolation

*Arabidopsis* GCPs were isolated enzymatically from leaves of 3- to 4-week-old plants according to previously reported procedures with some modifications (Ueno et al., 2005). Blended epidermal tissues were collected on 80  $\mu$ m nylon mesh, rinsed with cold sterile water, and incubated with first-step enzymatic digestion medium containing 0.5% (w/v) cellulase (Onozuka R-10; RPI Research Products International), 0.05% (w/v) macerozyme R-10 (PhytoTechnology Laboratories), 0.1% (w/v) polyvinylpyrrolidone, 0.2% (w/v) bovine serum albumin (BSA), 0.25 M mannitol, 1 mM  $\text{CaCl}_2$ , and 10 mM MES-KOH, pH 5.4 at 22°C for 1 h with 70 r.p.m. shaking. For the subsequent second-step enzymatic digestion, the epidermal tissues were incubated with 1.5% (w/v) cellulase RS (Onozuka RS; RPI Research Products International), 0.5% (w/v) macerozyme R-10 (PhytoTechnology Laboratories), 0.2% (w/v) BSA, 1 mM  $\text{CaCl}_2$ , and 0.4 M mannitol, pH 5.4 at 22°C for 1 h with 50 r.p.m. shaking. The digestion contents were passed through 80  $\mu$ m nylon mesh, and the filtrate was further passed through two layers of 10  $\mu$ m nylon mesh. The released GCPs were collected by centrifugation at 510 g for 12 min. The pellet was washed two times with 0.4 M mannitol with 1 mM  $\text{CaCl}_2$  and finally suspended in the same solution. The suspended GCPs were kept in the dark on ice until further use the following day.

### Phosphatase assays

AHA2 dephosphorylation assays were conducted as described by Spartz et al. (2014, 2017) using recombinant 6xHis-TRX-SAUR and -PP2C.D proteins and PM fractions prepared from AHA2-expressing yeast cells.

### RT-PCR

Primers used for semi-quantitative PCR of *PP2C.D* genes have been reported previously (Ren et al., 2018), except a different primer pair was used for *PP2C.D3* in this study as listed in Supplemental Table S1. Total RNA was prepared from rosette leaves or GCPs from 4-week-old plants using the Nucleospin RNA Plant (Macherey-Nagel) kit according to the manufacturer's instruction. On-column DNase treatment was performed to eliminate genomic DNA in RNA samples before cDNA synthesis using M-MLV reverse transcriptase (Promega). Semi-quantitative PCR was performed on the cDNAs using GoTaq DNA Polymerase (Promega) on a Techne TC-3000G PCR Thermal Cycler (GMI Inc.).

### Water loss assays and stomatal aperture measurement

For water loss assays, plants were acclimated to room humidity for 1 h prior to the experiment, or were assayed in the same walk-in growth room where they were growing. Age-matched rosette leaves were excised from 4-week-old plants and weighed using an analytical scale. Relative water loss was calculated based on the initial leaf weight at the 0 min time point. For stomatal aperture measurements, leaf epidermal peels were prepared from young expanded rosette leaves of 3-week-old plants, adhered onto a coverslip with silicone adhesive (Factor II, Inc. or Hollister Adapt 7730), and apertures examined as previously described with minor modifications (Azoulay-Shemer et al., 2015). Briefly, adhered epidermal peels were incubated in opening buffer (either 30 mM KCl, 10 mM MES, pH 6.1 or 10 mM KCl, 5 mM MES, 0.1 mM  $\text{CaCl}_2$ , pH 6.1) under white light for 3 h. For closing assays, peels were subsequently transferred to fresh opening buffer or to closing buffer (0.1 mM KCl, 8 mM  $\text{CaCl}_2$ , 10 mM MES titrated to pH 6.1 with  $\text{Ca(OH)}_2$ ) and transferred to darkness; or transferred to 10 mM KCl, 5 mM MES titrated to pH 6.1 with  $\text{Ca(OH)}_2$  and treated with ABA or solvent control. In an alternative protocol, full leaves or leaf halves with midveins removed were immersed in 30 mM KCl 10 mM MES opening buffer for 2 h in the light, and then treated with or without ABA in the light, or transferred to light or darkness, for 1 h before epidermal peels were made and imaged immediately. Both protocols gave similar results. Images of at least 45 stomata for each data point were captured using a Leica DM5000B or Zeiss Axio Imager A1 microscope. The stomatal aperture was calculated as the aperture width divided by the longitudinal length the same stomate. ImageJ software (<http://rsb.info.nih.gov/ij>) was used for the stomatal aperture measurement (Abramoff et al., 2004).

### Membrane fraction isolation, western, and far-western blot assays

Microsomal proteins of 7-d-old *Arabidopsis* seedlings grown on ATS plates containing 1% (w/v) sucrose were prepared as previously reported (Ito and Gray, 2006). Protein samples were separated on NuPage 4–12% acrylamide gels (Life Technologies) and blotted to nitrocellulose membranes. Blots were blocked with 5% (w/v) milk in TBS containing 0.1% (v/v) Tween-20 for 1 h and then incubated with antibodies or 0.1  $\mu$ M purified GST-14-3-3 (GF14 $\theta$ ) protein overnight at 4°C. GST-14-3-3 binding was subsequently detected using an  $\alpha$ -GST-HRP conjugate antibody (GE Healthcare) and chemiluminescence detection reagents (GE Healthcare) as previously described (Spartz et al., 2014).

### Bimolecular fluorescence complementation (BiFC)

BiFC assays were performed as previously described (Ren et al., 2018; Wong et al., 2019). Briefly, pSPYCE and pSPYNE expression constructs were infiltrated into approximately 5-week-old *Nicotiana benthamiana* leaves, and YFP fluorescence signals were observed 3-d post-infiltration using a



Nikon Ti2 A1si Confocal system (Nikon USA) with a 488 nm excitation wavelength and 545/40 nm emission filter.

### Gas exchange

Plants were grown in short-day conditions (8 h light/16 h dark cycle, 22°C/18°C, 70% relative humidity). Daylight regimes with steady 150  $\mu\text{mol m}^{-2} \text{s}^{-1}$  light intensity were used. Gas exchange measurements were carried out using the LI-COR 6400 XT Infrared Gas Analyzer (LICOR Biosciences) and a whole-plant Arabidopsis chamber (LI-COR 6400-17). Measurements were carried out at 22°C, 55% relative humidity, and at 400 p.p.m.  $\text{CO}_2$ . Gas exchange responses were measured using an external light source (LI-COR 6400-18) after the leaves were dark-adapted for 3 h. Measurements were carried out over the same period of the diurnal cycle and normalized to rosette area calculated using ImageJ (<http://rsb.info.nih.gov/ij>). The conductance curves for stomatal opening were fitted using the Marquardt-Levenberg algorithm of SigmaPlot v.11 (Systat, Cambridge USA) with Equations (1)–(3).

### Electrophysiology

Voltage clamp data were recorded from guard cells in epidermal peels using Henry's EP Software Suite (<http://www.psrg.org.uk>). Double-barreled microelectrodes (tip resistances > 100 M $\Omega$ ) were filled with 200 mM  $\text{K}^+$  acetate, pH 7.5 after equilibration against resin-bound BAPTA [1,2-bis(*o*-aminophenoxy)ethane-*N,N,N',N'*-tetraacetic acid] (Invitrogen) to prevent  $\text{Ca}^{2+}$  loading of the cytosol from the microelectrode as previously described (Blatt and Slayman, 1983; Blatt, 1987; Wang et al., 2013). Epidermal peels were pre-incubated in opening buffer (5 mM  $\text{Ca}^{2+}$ -MES, pH 6.1, with 60 mM KCl) for 1 h. Measurements were carried out in 5 mM  $\text{Ca}^{2+}$ -MES, pH 6.1, with 10 mM KCl. Surface areas of impaled guard cells were calculated assuming a spheroid geometry and voltages were analyzed using Henry's EP Software Suite (Blatt and Slayman, 1983; Wang et al., 2013). Where necessary for comparisons of lines between sets of experiments, data were referenced to the amplitudes of concurrent measurements from wild-type guard cells.

### Statistical analyses

All statistical analyses were done using JMP Pro 13.1 software suite (SAS Institute) to perform analysis of variance or otherwise mentioned in the text. The results were grouped under letters, with different letters showing significant differences ( $P < 0.05$ ) based on Tukey's HSD (honestly significant difference) test.

### Accession numbers

All sequence data can be found in the GenBank/EMBL data libraries under the following accession numbers: *PP2C.D1* (At5g02760), *PP2C.D2* (At3g17090), *PP2C.D3* (At3g12620), *PP2C.D4* (At3g55050), *PP2C.D5* (At4g38520), *PP2C.D6* (At3g51370), *PP2C.D7* (At5g66080), *PP2C.D8* (At4g33920), *PP2C.D9* (At5g06750), *SAUR19* (At5g18010), *SAUR56*

(At1g76190), *SAUR60* (At1g20470), *SAUR63* (At1g29440), *ACTIN7* (At5g09810).

### Supplemental data

The following materials are available in the online version of this article.

**Supplemental Figure S1** Stomatal aperture measurements of *SAUR19* and *SAUR63* gain-of-function lines.

**Supplemental Figure S2** *SAUR56* and *SAUR60* are expressed in guard cells and regulate stomatal aperture.

**Supplemental Figure S3** Expression of *PP2C.D* genes in guard cells.

**Supplemental Figure S4** Water loss assay of *pp2c.d* mutants and complementation lines.

**Supplemental Figure S5** Guard cell overexpression of *PP2C.D2-RFP* and *PP2C.D6-RFP*.

**Supplemental Figure S6** *SAUR56* and *SAUR60* interact with *PP2C.D* proteins in BiFC assays.

**Supplemental Figure S7** Loss-of-function alleles of *SAUR56* and *SAUR60*.

**Supplemental Figure S8** Characteristics of  $\text{K}_{\text{out}}^+$  and  $\text{K}_{\text{in}}^+$  channels in guard cells of *SAUR* overexpression plants.

**Supplemental Table S1** Oligonucleotides used in this study.

### Acknowledgments

We thank Dr Masaki Okumura for his helpful advice on the isolation of Arabidopsis GCPs and Dr Nathalie Leonhardt for providing the ABA-insensitive *MYB60* promoter derivative used to construct the V400/W008 expression vector. We also thank the UM College of Biological Sciences Imaging Center for assistance with confocal microscopy.

### Funding

This work was supported by the National Science Foundation (MCB-1613809 to W.M.G., MCB-1615557 to J.W.R.); the Biotechnology and Biological Sciences Research Council (BB/P011586/1 to M.R.B.); the National Institutes of Health (GM067203 to W.M.G.); and a Summer Undergraduate Research Fellowship from the UNC Office of Undergraduate Research to B.W.

### References

- Abramoff MD, Magelhaes PJ, Ram SJ (2004) Image processing with ImageJ. *Biophotonics Int* **11**: 36–42
- Adrian J, Chang J, Ballenger CE, Bargmann BO, Alassimone J, Davies KA, Lau OS, Matos JL, Hachez C, Lanctot A, et al. (2015) Transcriptome dynamics of the stomatal lineage: birth, amplification, and termination of a self-renewing population. *Dev Cell* **33**: 107–118
- Akimoto-Tomiya C, Furutani A, Tsuge S, Washington EJ, Nishizawa Y, Minami E, Ochiai H (2012) XopR, a type III effector secreted by *Xanthomonas oryzae* pv. *oryzae*, suppresses microbe-associated molecular pattern-triggered immunity in *Arabidopsis thaliana*. *Mol Plant Microbe Interact* **25**: 505–514
- Ando E, Kinoshita T (2018) Red light-induced phosphorylation of plasma membrane H. *Plant Physiol* **178**: 838–849



- Azoulay-Shemer T, Palomares A, Bagheri A, Israelsson-Nordstrom M, Engineer CB, Bargmann BO, Stephan AB, Schroeder JI** (2015) Guard cell photosynthesis is critical for stomatal turgor production, yet does not directly mediate CO<sub>2</sub>- and ABA-induced stomatal closing. *Plant J* **83**: 567–581
- Bauer H, Ache P, Lautner S, Fromm J, Hartung W, Al-Rasheid KA, Sonnewald S, Sonnewald U, Kneitz S, Lachmann N, et al.** (2013) The stomatal response to reduced relative humidity requires guard cell-autonomous ABA synthesis. *Curr Biol* **23**: 53–57
- Blatt MR** (1987) Electrical characteristics of stomatal guard cells: the ionic basis of the membrane potential and the consequence of potassium chlorides leakage from microelectrodes. *Planta* **170**: 272–287
- Blatt MR** (1990) Potassium channel currents in intact stomatal guard cells: rapid enhancement by abscisic acid. *Planta* **180**: 445–455
- Blatt MR, Armstrong F** (1993) K<sup>+</sup> channels of stomatal guard cells: abscisic acid-evoked control of the outward rectifier mediated by cytoplasmic pH. *Planta* **191**: 330–341
- Blatt MR, Clint GM** (1989) Mechanisms of fusicoccin action: kinetic modification and inactivation of K(+) channels in guard cells. *Planta* **178**: 509–523
- Blatt MR, Slayman CL** (1983) KCl leakage from microelectrodes and its impact on the membrane parameters of a nonexcitable cell. *J Membr Biol* **72**: 223–234
- Blatt MR, Slayman CL** (1987) Role of “active” potassium transport in the regulation of cytoplasmic pH by nonanimal cells. *Proc Natl Acad Sci U S A* **84**: 2737–2741
- Chae K, Isaacs CG, Reeves PH, Maloney GS, Muday GK, Nagpal P, Reed JW** (2012) Arabidopsis SMALL AUXIN UP RNA63 promotes hypocotyl and stamen filament elongation. *Plant J* **71**: 684–697
- Chen ZH, Hills A, Bätz U, Amtmann A, Lew VL, Blatt MR** (2012) Systems dynamic modeling of the stomatal guard cell predicts emergent behaviors in transport, signaling, and volume control. *Plant Physiol* **159**: 1235–1251
- Chen ZH, Hills A, Lim CK, Blatt MR** (2010) Dynamic regulation of guard cell anion channels by cytosolic free Ca<sub>2</sub><sup>+</sup> concentration and protein phosphorylation. *Plant J* **61**: 816–825
- Chiu J, March PE, Lee R, Tillett D** (2004) Site-directed, ligase-independent mutagenesis (SLIM): a single-tube methodology approaching 100% efficiency in 4 h. *Nucleic Acids Res* **32**: e174
- Clough SJ, Bent AF** (1998) Floral dip: a simplified method for Agrobacterium-mediated transformation of Arabidopsis thaliana. *Plant J* **16**: 735–743
- Cominelli E, Galbiati M, Albertini A, Fornara F, Conti L, Coupland G, Tonelli C** (2011) DOF-binding sites additively contribute to guard cell-specificity of AtMYB60 promoter. *BMC Plant Biol* **11**: 162
- Cominelli E, Galbiati M, Vavasseur A, Conti L, Sala T, Vuylsteke M, Leonhardt N, Dellaporta SL, Tonelli C** (2005) A guard-cell-specific MYB transcription factor regulates stomatal movements and plant drought tolerance. *Curr Biol* **15**: 1196–1200
- Curtis MD, Grossniklaus U** (2003) A gateway cloning vector set for high-throughput functional analysis of genes in planta. *Plant Physiol* **133**: 462–469
- Du M, Spalding EP, Gray WM** (2020) Rapid auxin-mediated cell expansion. *Annu Rev Plant Biol* **71**: 379–402
- Earley KW, Haag JR, Pontes O, Opper K, Juehne T, Song K, Pikaard CS** (2006) Gateway-compatible vectors for plant functional genomics and proteomics. *Plant J* **45**: 616–629
- Fuglsang AT, Visconti S, Drumm K, Jahn T, Stensballe A, Mattei B, Jensen ON, Aducci P, Palmgren MG** (1999) Binding of 14-3-3 protein to the plasma membrane H(+)-ATPase AHA2 involves the three C-terminal residues Tyr(946)-Thr-Val and requires phosphorylation of Thr(947). *J Biol Chem* **274**: 36774–36780
- García-Mata C, Gay R, Sokolovski S, Hills A, Lamattina L, Blatt MR** (2003) Nitric oxide regulates K<sup>+</sup> and Cl<sup>-</sup> channels in guard cells through a subset of abscisic acid-evoked signaling pathways. *Proc Natl Acad Sci U S A* **100**: 11116–11121
- Geiger D, Scherzer S, Mumm P, Stange A, Marten I, Bauer H, Ache P, Matschi S, Liese A, Al-Rasheid KA, et al.** (2009) Activity of guard cell anion channel SLAC1 is controlled by drought-stress signaling kinase-phosphatase pair. *Proc Natl Acad Sci USA* **106**: 21425–21430
- Grabov A, Blatt MR** (1997) Parallel control of the inward-rectifier K<sup>+</sup> channel by cytosolic-free Ca<sup>2+</sup> and pH in Vicia guard cells. *Planta* **201**: 84–95
- Grabov A, Blatt MR** (1998) Membrane voltage initiates Ca<sup>2+</sup> waves and potentiates Ca<sup>2+</sup> increases with abscisic acid in stomatal guard cells. *Proc Natl Acad Sci USA* **95**: 4778–4783
- Grabov A, Blatt MR** (1999) A steep dependence of inward-rectifying potassium channels on cytosolic free calcium concentration increase evoked by hyperpolarization in guard cells. *Plant Physiol* **119**: 277–288
- Hamilton DW, Hills A, Kohler B, Blatt MR** (2000) Ca<sup>2+</sup> channels at the plasma membrane of stomatal guard cells are activated by hyperpolarization and abscisic acid. *Proc Natl Acad Sci USA* **97**: 4967–4972
- Hayashi Y, Nakamura S, Takemiya A, Takahashi Y, Shimazaki K, Kinoshita T** (2010) Biochemical characterization of in vitro phosphorylation and dephosphorylation of the plasma membrane H<sup>+</sup>-ATPase. *Plant Cell Physiol* **51**: 1186–1196
- Hills A, Chen ZH, Amtmann A, Blatt MR, Lew VL** (2012) OnGuard, a computational platform for quantitative kinetic modeling of guard cell physiology. *Plant Physiol* **159**: 1026–1042
- Hosy E, Vavasseur A, Mouline K, Dreyer I, Gaymard F, Poree F, Boucherez J, Lebaudy A, Bouchez D, Very AA, et al.** (2003) The Arabidopsis outward K<sup>+</sup> channel GORK is involved in regulation of stomatal movements and plant transpiration. *Proc Natl Acad Sci USA* **100**: 5549–5554
- Inoue SI, Kinoshita T** (2017) Blue light regulation of stomatal opening and the plasma membrane H. *Plant Physiol* **174**: 531–538
- Ito H, Gray WM** (2006) A gain-of-function mutation in the Arabidopsis pleiotropic drug resistance transporter PDR9 confers resistance to auxinic herbicides. *Plant Physiol* **142**: 63–74
- Jezek M, Blatt MR** (2017) The membrane transport system of the guard cell and its integration for stomatal dynamics. *Plant Physiol* **174**: 487–519
- Karimi M, Inzé D, Depicker A** (2002) GATEWAY vectors for Agrobacterium-mediated plant transformation. *Trends Plant Sci* **7**: 193–195
- Kinoshita T, Shimazaki K** (1999) Blue light activates the plasma membrane H(+)-ATPase by phosphorylation of the C-terminus in stomatal guard cells. *EMBO J* **18**: 5548–5558
- Lebaudy A, Vavasseur A, Hosy E, Dreyer I, Leonhardt N, Thibaud JB, Véry AA, Simonneau T, Sentenac H** (2008) Plant adaptation to fluctuating environment and biomass production are strongly dependent on guard cell potassium channels. *Proc Natl Acad Sci USA* **105**: 5271–5276
- Lefoulon C, Waghmare S, Karnik R, Blatt MR** (2018) Gating control and K(+) uptake by the KAT1 K(+) channel leveraged through membrane anchoring of the trafficking protein SYP121. *Plant Cell Environ* **41**: 2668–2677
- Linder B, Raschke K** (1992) A slow anion channel in guard cells, activating at large hyperpolarization, may be principal for stomatal closing. *FEBS Lett* **313**: 27–30
- Maathuis FJ, Sanders D** (1994) Mechanism of high-affinity potassium uptake in roots of Arabidopsis thaliana. *Proc Natl Acad Sci USA* **91**: 9272–9276
- Merlot S, Leonhardt N, Fenzi F, Valon C, Costa M, Piette L, Vavasseur A, Genty B, Boivin K, Müller A, Giraudat J, Leung J** (2007) Constitutive activation of a plasma membrane H(+)-ATPase prevents abscisic acid-mediated stomatal closure. *EMBO J* **26**: 3216–3226

- Meyer S, Mumm P, Imes D, Endler A, Weder B, Al-Rasheid KA, Geiger D, Marten I, Martinoia E, Hedrich R (2010) AtALMT12 represents an R-type anion channel required for stomatal movement in Arabidopsis guard cells. *Plant J* **63**: 1054–1062
- Minguet-Parramona C, Wang Y, Hills A, Vialet-Chabrand S, Griffiths H, Rogers S, Lawson T, Lew VL, Blatt MR (2016) An optimal frequency in Ca<sup>2+</sup> oscillations for stomatal closure is an emergent property of ion transport in guard cells. *Plant Physiol* **170**: 33–42
- Nakagawa T, Kurose T, Hino T, Tanaka K, Kawamukai M, Niwa Y, Toyooka K, Matsuoka K, Jinbo T, Kimura T (2007) Development of series of gateway binary vectors, pGWBs, for realizing efficient construction of fusion genes for plant transformation. *J Biosci Bioeng* **104**: 34–41
- Nakamura RL, McKendree WL, Hirsch RE, Sedbrook JC, Gaber RF, Sussman MR (1995) Expression of an Arabidopsis potassium channel gene in guard cells. *Plant Physiol* **109**: 371–374
- Olsson A, Svennelid F, Ek B, Sommarin M, Larsson C (1998) A phosphothreonine residue at the C-terminal end of the plasma membrane H<sup>+</sup>-ATPase is protected by fusicoccin-induced 14-3-3 binding. *Plant Physiol* **118**: 551–555
- Osakabe Y, Arinaga N, Umezawa T, Katsura S, Nagamachi K, Tanaka H, Ohiraki H, Yamada K, Seo SU, Abo M, et al. (2013) Osmotic stress responses and plant growth controlled by potassium transporters in Arabidopsis. *Plant Cell* **25**: 609–624
- Peterson BA, Haak DC, Nishimura MT, Teixeira PJ, James SR, Dangi JL, Nimchuk ZL (2016) Genome-wide assessment of efficiency and specificity in CRISPR/Cas9 mediated multiple site targeting in Arabidopsis. *PLoS One* **11**: e0162169
- Pilot G, Gaymard F, Mouline K, Chérel I, Sentenac H (2003) Regulated expression of Arabidopsis shaker K<sup>+</sup> channel genes involved in K<sup>+</sup> uptake and distribution in the plant. *Plant Mol Biol* **51**: 773–787
- Pilot G, Lacombe B, Gaymard F, Chérel I, Boucherez J, Thibaud JB, Sentenac H (2001) Guard cell inward K<sup>+</sup> channel activity in Arabidopsis involves expression of the twin channel subunits KAT1 and KAT2. *J Biol Chem* **276**: 3215–3221
- Ren H, Gray WM (2015) SAUR Proteins as Effectors of Hormonal and Environmental Signals in Plant Growth. *Mol Plant* **8**: 1153–1164
- Ren H, Park MY, Spartz AK, Wong JH, Gray WM (2018) A subset of plasma membrane-localized PP2C.D phosphatases negatively regulate SAUR-mediated cell expansion in Arabidopsis. *PLoS Genet* **14**: e1007455
- Schmidt C, Schelle I, Liao YJ, Schroeder JI (1995) Strong regulation of slow anion channels and abscisic acid signaling in guard cells by phosphorylation and dephosphorylation events. *Proc Natl Acad Sci USA* **92**: 9535–9539
- Spartz AK, Lee SH, Wenger JP, Gonzalez N, Itoh H, Inzé D, Peer WA, Murphy AS, Overvoorde PJ, Gray WM (2012) The SAUR19 subfamily of SMALL AUXIN UP RNA genes promote cell expansion. *Plant J* **70**: 978–990
- Spartz AK, Lor VS, Ren H, Olszewski NE, Miller ND, Wu G, Spalding EP, Gray WM (2017) Constitutive expression of Arabidopsis SMALL AUXIN UP RNA19 (SAUR19) in tomato confers auxin-independent hypocotyl elongation. *Plant Physiol* **173**: 1453–1462
- Spartz AK, Ren H, Park MY, Grandt KN, Lee SH, Murphy AS, Sussman MR, Overvoorde PJ, Gray WM (2014) SAUR inhibition of PP2C-D phosphatases activates plasma membrane H<sup>+</sup>-ATPases to promote cell expansion in Arabidopsis. *Plant Cell* **26**: 2129–2142
- Suhita D, Raghavendra AS, Kwak JM, Vavasseur A (2004) Cytoplasmic alkalization precedes reactive oxygen species production during methyl jasmonate- and abscisic acid-induced stomatal closure. *Plant Physiol* **134**: 1536–1545
- Sun N, Wang J, Gao Z, Dong J, He H, Terzaghi W, Wei N, Deng XW, Chen H (2016) Arabidopsis SAURs are critical for differential light regulation of the development of various organs. *Proc Natl Acad Sci USA* **113**: 6071–6076
- Svennelid F, Olsson A, Piotrowski M, Rosenquist M, Ottman C, Larsson C, Oecking C, Sommarin M (1999) Phosphorylation of Thr-948 at the C terminus of the plasma membrane H<sup>+</sup>-ATPase creates a binding site for the regulatory 14-3-3 protein. *Plant Cell* **11**: 2379–2391
- Tovar-Mendez A, Miernyk JA, Hoyos E, Randall DD (2014) A functional genomic analysis of Arabidopsis thaliana PP2C clade D. *Protoplasma* **251**: 265–271
- Ueno K, Kinoshita T, Inoue S, Emi T, Shimazaki K (2005) Biochemical characterization of plasma membrane H<sup>+</sup>-ATPase activation in guard cell protoplasts of Arabidopsis thaliana in response to blue light. *Plant Cell Physiol* **46**: 955–963
- Véry AA, Nieves-Cordones M, Daly M, Khan I, Fizames C, Sentenac H (2014) Molecular biology of K<sup>+</sup> transport across the plant cell membrane: what do we learn from comparison between plant species? *J Plant Physiol* **171**: 748–769
- Wang RS, Pandey S, Li S, Gookin TE, Zhao Z, Albert R, Assmann SM (2011) Common and unique elements of the ABA-regulated transcriptome of Arabidopsis guard cells. *BMC Genomics* **12**: 216
- Wang Y, Chen ZH, Zhang B, Hills A, Blatt MR (2013) PYR/PYL/RCAR abscisic acid receptors regulate K<sup>+</sup> and Cl<sup>-</sup> channels through reactive oxygen species-mediated activation of Ca<sup>2+</sup> channels at the plasma membrane of intact Arabidopsis guard cells. *Plant Physiol* **163**: 566–577
- Wang Y, Hills A, Vialet-Chabrand S, Papanatsiou M, Griffiths H, Rogers S, Lawson T, Lew VL, Blatt MR (2017) Unexpected connections between humidity and ion transport discovered using a model to bridge guard cell-to-leaf scales. *Plant Cell* **29**: 2921–2939
- Wang Y, Noguchi K, Ono N, Inoue S, Terashima I, Kinoshita T (2014) Overexpression of plasma membrane H<sup>+</sup>-ATPase in guard cells promotes light-induced stomatal opening and enhances plant growth. *Proc Natl Acad Sci USA* **111**: 533–538
- Wang Y, Papanatsiou M, Eisenach C, Karnik R, Williams M, Hills A, Lew VL, Blatt MR (2012) Systems dynamic modeling of a guard cell Cl<sup>-</sup> channel mutant uncovers an emergent homeostatic network regulating stomatal transpiration. *Plant Physiol* **160**: 1956–1967
- Wong JH, Spartz AK, Park MY, Du M, Gray WM (2019) Mutation of a conserved motif of PP2C.D phosphatases confers SAUR immunity and constitutive activity. *Plant Physiol* **181**: 353–366
- Yamauchi S, Takemiya A, Sakamoto T, Kurata T, Tsutsumi T, Kinoshita T, Shimazaki K (2016) The plasma membrane H<sup>+</sup>-ATPase AHA1 plays a major role in stomatal opening in response to blue light. *Plant Physiol* **171**: 2731–2743
- Yang Y, Costa A, Leonhardt N, Siegel RS, Schroeder JI (2008) Isolation of a strong Arabidopsis guard cell promoter and its potential as a research tool. *Plant Methods* **4**: 6